

# Lepton-flavour violation in a Pati-Salam model with gauged flavour symmetry

Thorsten Feldmann<sup>\*</sup>, Christoph Luhn<sup>†</sup>, Paul Moch<sup>‡</sup>

*Theoretische Physik 1, Naturwissenschaftlich-Technische Fakultät, Universität Siegen,  
Walter-Flex-Straße 3, 57068 Siegen, Germany*

## Abstract

Combining Pati-Salam (PS) and flavour symmetries in a renormalisable setup, we devise a scenario which produces realistic masses for the charged leptons. Flavour-symmetry breaking scalar fields in the adjoint representations of the PS gauge group are responsible for generating different flavour structures for up- and down-type quarks as well as for leptons. The model is characterised by new heavy fermions which mix with the Standard Model quarks and leptons. In particular, the partners for the third fermion generation induce sizeable sources of flavour violation. Focusing on the charged-lepton sector, we scrutinise the model with respect to its implications for lepton-flavour violating processes such as  $\mu \rightarrow e\gamma$ ,  $\mu \rightarrow 3e$  and muon conversion in nuclei.

---

<sup>\*</sup>E-mail: [thorsten.feldmann@uni-siegen.de](mailto:thorsten.feldmann@uni-siegen.de)

<sup>†</sup>E-mail: [christoph.luhn@uni-siegen.de](mailto:christoph.luhn@uni-siegen.de)

<sup>‡</sup>E-mail: [paulmoch@physik.uni-siegen.de](mailto:paulmoch@physik.uni-siegen.de)

# 1 Introduction

The successful description of gauge interactions is arguably one of the most attractive features of the Standard Model (SM) of particle physics. Their structure is dictated by the symmetry  $SU(3) \times SU(2) \times U(1)$ , where each factor comes with its own gauge coupling constant. Adding to this the electroweak symmetry breaking sector introduces two extra parameters, the vacuum expectation value (VEV) and the mass of the Higgs boson, discovered at the LHC in 2012 [1, 2]. Unlike the gauge interactions, the structure of the Yukawa sector, which provides the seed of quark and lepton masses and mixing, is much less understood. Ever since I. I. Rabi phrased his old question about the muon, “Who ordered it?”, physicists have been trying hard to unravel the origin of flavour.

Strictly speaking, the flavour structure of the SM does not require an underlying principle. Assigning appropriate numerical values to the a priori undetermined Yukawa coupling constants is sufficient to consistently parameterise flavour in the SM. Yet, when considering extensions of the SM, the need for a theory of flavour becomes more pressing. In general, the implications of theories beyond the SM for low-energy physics can be formulated using the SM effective field theory approach, with a total of 2499 possible operators at dimension six [3–5]. Many of these non-renormalisable operators entail new sources of flavour and CP violation. Without a mechanism that controls the size and the structure of these new couplings, the effective theory would generally not be compatible with experimental results for certain flavour observables [6].

Although not a theory of flavour, the concept of minimal flavour violation (MFV) provides an appealing framework for constructing higher-dimensional operators which efficiently suppresses flavour changing processes beyond the SM [7–11]. The idea is based on a symmetry principle, more precisely on the maximal flavour symmetry of the SM in the absence of the Yukawa couplings. As each of the five fermionic SM multiplets comes in three generations, it is given by  $U(3)^5$ . Furthermore, MFV postulates that the only flavour symmetry breaking entities are the Yukawa matrices themselves, whose occurrence in the higher-dimensional operators of an effective field theory is controlled by the original flavour symmetry.

In order to embed the concept of MFV into a high-energy theory, it is necessary to promote the Yukawa matrices to scalar fields. In such a setup, the SM Yukawa couplings originate dynamically from non-renormalisable operators after inserting VEVs for the matrix-valued scalar flavon fields. Sequential flavour symmetry breaking [12] can be realised by hierarchical vacuum configurations which are derived from appropriate flavour symmetric potentials as discussed e.g. in [13–21]. Massless Goldstone modes are avoided by gauging the flavour symmetry. Pursuing this idea in a renormalisable setup, Grinstein, Redi and Villadoro (GRV) proposed a model [22] in which new heavy partners of the SM fermions mediate the coupling of left- and right-chiral quarks and leptons to the Higgs, with the resulting effective Yukawa matrices being inversely proportional to the VEVs of the matrix-valued flavon fields. The extension of the fermionic particle content was chosen such as to cancel all gauge anomalies of the SM and flavour symmetries (see also [23]).

The basic idea of GRV has been extended and applied in the context of the SM [24, 25], grand unified theories (GUTs) [26–29], and supersymmetric theories [30, 31]. The combination of flavour and GUT symmetries is of particular interest as it allows to unify the

theory both horizontally (by organising the three generations of fermions into triplets) as well as vertically (by combining independent SM multiplets into a single GUT multiplet). For reviews, see e.g. [32–39]. Among the various GUT symmetries, the Pati-Salam (PS) gauge symmetry [40, 41] provides a rich playground in which gauge coupling unification can be realised via several intermediate mass scales [42–49]. Flavour models which are compatible with an underlying PS gauge group have been constructed abundantly in the literature, see e.g. [50–61]. A concrete setup which embeds the GRV mechanism in an explicit left-right (i.e.  $Z_2$ ) symmetric PS GUT was put forth in [29]. With all SM multiplets (plus the right-chiral neutrino) being unified into only two PS multiplets, the full symmetry of the Lagrangian is given by

$$\underbrace{\left( SU(4) \times SU(2) \times SU(2)' \right)}_{\text{Pati-Salam}} \times \underbrace{\left( SU(3)_I \times SU(3)_{II} \right)}_{\text{flavour}} \times Z_2 ,$$

where the  $Z_2$  maps the multiplet  $(\omega_c, \omega, \omega')(\omega_I, \omega_{II})$  into  $(\bar{\omega}_c, \omega', \omega)(\bar{\omega}_{II}, \bar{\omega}_I)$ . As in [29], we assume that the  $U(1)$  factors within  $U(3)_I \times U(3)_{II}$  are explicitly broken in the scalar potential, e.g. by terms involving the determinant of the matrix-valued flavons.

While the phenomenology of the quark sector was investigated thoroughly for this setup, the study in [29] stopped short of a similar analysis of the lepton sector. It is the purpose of the present article to complete this work by formulating a viable extension of the lepton sector, involving additional Pati-Salam and flavour-symmetry breaking scalar flavon fields, and studying the expected signatures for lepton-flavour violating (LFV) processes.

The layout of the remainder of this paper is as follows. In Section 2, we recapitulate the main ingredients of the model in [29] and present the extension of the scalar sector necessary to generate viable charged-lepton masses. Section 3 discusses the diagonalisation of the charged- and neutral-lepton mass matrices, as well as the effect this change of basis has on the gauge-kinetic terms. We explicitly state the resulting anomalous couplings of the leptons to the electroweak gauge bosons  $W$  and  $Z$ , briefly also commenting on the anomalous Higgs coupling. In Section 4, we relate these anomalous couplings to the LFV observables  $\mu \rightarrow e\gamma$ ,  $\mu \rightarrow 3e$  and muon conversion in the vicinity of nuclei. The phenomenological implications of our model as derived from a numerical parameter scan are discussed in Section 5. We conclude in Section 6. Appendix A provides technical details on the transformation from the flavour basis to the mass basis.

## 2 A Pati-Salam model with viable charged leptons

The setup of the left-right symmetric Pati-Salam model with gauged  $SU(3)_I \times SU(3)_{II}$  flavour symmetry has been discussed in [29]. In order to make the present paper self-contained, we begin with a brief recapitulation of the main ideas and the required ingredients of the model. The left- and right-chiral Pati-Salam multiplets  $q_{L,R}$  contain all SM fermions. Additional fermionic partners  $(\Sigma_{L,R}, \Xi_{L,R})$  are introduced in order to formulate a renormalisable model in which the flavour symmetry is broken by VEVs of matrix-valued scalar fields  $S$  and  $T'$ . These flavon fields transform trivially under PS, except

for  $T'$  which furnishes a triplet representation of the PS gauge factor  $SU(2)'$ . The combination of flavons in both the singlet and triplet representation of  $SU(2)'$  is necessary to distinguish up-type from down-type flavour structures. To first approximation, the Yukawa matrices of the light (i.e. SM) fermions are obtained by integrating out the heavy partners. More accurately, it is necessary to diagonalise a  $9 \times 9$  mass matrix in order to identify the correct mass eigenstates. This is particularly relevant for the up-type sector where the two partners of the top quark are only marginally heavier than the top itself.

As with every gauge symmetry, anomaly considerations put severe constraints on the fermionic particle content of the model. The resulting need for introducing further fermions in our PS setup can be naturally combined with the construction of a realistic (Majorana) neutrino sector. To this end, we introduce PS neutral fermions  $\Theta_{L,R}$  which acquire Majorana masses through extra scalars  $S_\nu^{(\prime)}$ . As a side effect, these additional flavour symmetry breaking scalar fields are responsible for decoupling the flavour gauge bosons from low-energy physics. The coupling of  $\Theta_L$  to the neutral component of  $\Sigma_R$  induces a heavy Majorana mass for the latter, which in turn generates light neutrino masses via the seesaw mechanism. We refer the reader to [29] for further details on the construction of the model.

The complete particle content of the Pati-Salam model as defined in [29] is shown in Table 1. It yields a renormalisable Yukawa Lagrangian of the form

$$\mathcal{L}_{\text{Yuk}} = \mathcal{L}_{\text{Yuk}}^q + \mathcal{L}_{\text{Yuk}}^\nu, \quad (2.1)$$

with

$$\begin{aligned} \mathcal{L}_{\text{Yuk}}^q = & \lambda \bar{q}_L H \Sigma_R + \bar{\Sigma}_L (\kappa_S S + \kappa_T T') \Sigma_R + M \bar{\Sigma}_L q_R + \text{h.c.} \\ & + \lambda \bar{\Xi}_L H q_R + \bar{\Xi}_L (\kappa_S S + \kappa_T T) \Xi_R + M \bar{q}_L \Xi_R + \text{h.c.}, \end{aligned} \quad (2.2)$$

and

$$\begin{aligned} \mathcal{L}_{\text{Yuk}}^\nu \sim & \bar{\Theta}_L \Phi' \Sigma_R + \frac{1}{2} \bar{\Theta}_L S_\nu \bar{\Theta}_L + \text{h.c.} \\ & + \bar{\Xi}_L \Phi \Theta_R + \frac{1}{2} \Theta_R S'_\nu \Theta_R + \text{h.c.} \\ & + \bar{\Theta}_L S^\dagger \Theta_R + \text{h.c.} \end{aligned} \quad (2.3)$$

The Lagrangian in Eq. (2.2) describes the Yukawa structure of the charged fermions. A comprehensive discussion of the quark sector can be found in [29]. Turning to the charged leptons, we observe that the effective Yukawa matrix  $Y_\ell$  is identical to the down-type quark Yukawa matrix  $Y_d$ . Although this provides a reasonable first approximation, it is clear that an extension of some sort is required to accommodate a fully realistic fermion mass pattern. We have already outlined one such possibility in Appendix A.2 of [29], and it is the purpose of this paper to work out the lepton-flavour phenomenology of such an extension.

The idea consists in enlarging the scalar sector by flavour symmetry breaking flavon fields which transform in the adjoint representation of  $SU(4)$ , i.e. in the **15**. Hence we have additionally included  $S_{15}$  and  $T_{15}^{(\prime)}$  in Table 1, where the transformation properties are identical to  $S$  and  $T^{(\prime)}$  of the original model with the exception of  $SU(4)$ . Since the original

	Pati-Salam Symmetry $SU(4) \times SU(2) \times SU(2)'$	Flavour Symmetry $SU(3)_I \times SU(3)_{II}$	VEV
$\bar{q}_L$	$(\bar{4}, 2, 1)$	$(\bar{3}, 1)$	—
$q_R$	$(4, 1, 2)$	$(1, 3)$	—
$H$	$(1, 2, 2)$	$(1, 1)$	$v_{u,d}$
$\bar{\Sigma}_L$	$(\bar{4}, 1, 2)$	$(1, \bar{3})$	—
$\Sigma_R$	$(4, 1, 2)$	$(3, 1)$	—
$\bar{\Xi}_L$	$(\bar{4}, 2, 1)$	$(1, \bar{3})$	—
$\Xi_R$	$(4, 2, 1)$	$(3, 1)$	—
$T_{1,15}$	$(1 + 15, 3, 1)$	$(\bar{3}, 3)$	0
$T'_{1,15}$	$(1 + 15, 1, 3)$	$(\bar{3}, 3)$	$t'_{1,15} M$
$S_{1,15}$	$(1 + 15, 1, 1)$	$(\bar{3}, 3)$	$s_{1,15} M$
$\bar{\Theta}_L$	$(1, 1, 1)$	$(\bar{3}, 8)$	—
$\Theta_R$	$(1, 1, 1)$	$(8, 3)$	—
$S_\nu$	$(1, 1, 1)$	$(6, 1)$	$s_\nu \Lambda_\nu$
$S'_\nu$	$(1, 1, 1)$	$(1, \bar{6})$	$s'_\nu \Lambda_\nu$
$\Phi$	$(4, 2, 1)$	$(8, 1)$	0
$\Phi'$	$(\bar{4}, 1, 2)$	$(1, 8)$	$\varphi' \Lambda_\varphi$

Table 1: The particle content of the Pati-Salam model with imposed flavour symmetry as defined in [29] and augmented by flavon fields in the adjoint representation of  $SU(4)$ . Left- and right-chiral fermions  $\psi_{L,R}$  are denoted by subscripts  $L$  and  $R$ , respectively. The VEVs of the scalar fields are given in the rightmost column. The lower part of the table shows fields necessary for generating Majorana neutrino masses.

flavon fields were taken to be  $SU(4)$  singlets, we have written  $S_1 = S$  and  $T_1^{(\prime)} = T^{(\prime)}$ . The resulting changes to the Yukawa interactions are given by simple replacements in Eq. (2.2) such as for instance<sup>1</sup>

$$\bar{\Sigma}_L (\kappa_S S) \Sigma_R \rightarrow \bar{\Sigma}_L (\kappa_{S_1} S_1 + \kappa_{S_{15}} S_{15}) \Sigma_R. \quad (2.4)$$

Inserting the flavon VEVs and dividing by the new-physics (NP) mass scale  $M$ , we can define dimensionless  $3 \times 3$  matrices  $s_i = \kappa_{S_i} \langle S_i \rangle / M$ . The presence of the adjoint entails a difference between quarks and leptons: the  $SU(3)$  conserving direction of the **15**, written as a matrix, is  $\text{Diag}(1, 1, 1, -3)$  so that the leptons pick up a relative factor of  $-3$  compared to the quarks.<sup>2</sup> Hence we are led to the following replacements

$$\begin{aligned} \text{quarks:} \quad s &\rightarrow s_q \equiv s_1 + s_{15}, & t' &\rightarrow t'_q \equiv t'_1 + t'_{15}, \\ \text{leptons:} \quad s &\rightarrow s_l \equiv s_1 - 3 s_{15}, & t' &\rightarrow t'_l \equiv t'_1 - 3 t'_{15}. \end{aligned} \quad (2.5)$$

<sup>1</sup>Note that only  $S_1^\dagger$  can couple in the term of the third line of Eq. (2.3).

<sup>2</sup>This so-called Georgi-Jarlskog factor was first discussed in the context of  $SU(5)$  in [62], where the scalar sector was enlarged by a Higgs multiplet in the **45** which (contrary to the standard Higgs in the **5**) treats quarks and leptons differently.

A setup where all  $SU(4)$  singlet flavon fields are accompanied by flavons in the adjoint of  $SU(4)$  therefore decouples the flavour structure of the quark and lepton sector completely. Having discussed the phenomenology of the quark sector extensively in [29], we focus exclusively on the leptons in the following. However, we do not pursue a numerical fit to neutrino oscillation data because the implementation of light Majorana neutrino masses in our model introduces the independent flavour structure of  $\langle S_\nu \rangle$  so that a realistic PMNS mixing matrix can always be achieved regardless of quark and charged-lepton flavour.

Analogously to the quark sector, bilinear mass terms of the charged leptons, including their heavy partners, can be expressed in terms of a  $9 \times 9$  matrix. Defining the basis<sup>3</sup>

$$\overline{\Psi}_L^\ell \equiv (\overline{q}_L^\ell, \overline{\Sigma}_L^\ell, \overline{\Xi}_L^\ell), \quad \Psi_R^\ell \equiv (q_R^\ell, \Sigma_R^\ell, \Xi_R^\ell), \quad (2.6)$$

we have

$$\mathcal{M}^\ell = \begin{pmatrix} 0 & \mathbb{1} \lambda \epsilon_d & \mathbb{1} \\ \mathbb{1} & s_l - t'_l & 0 \\ \mathbb{1} \lambda \epsilon_d & 0 & s_l \end{pmatrix} M, \quad (2.7)$$

where

$$\epsilon_d \equiv \frac{v_d}{\sqrt{2} M} = \frac{v}{\sqrt{2} \sqrt{1 + \tan^2 \beta} M}, \quad (2.8)$$

and  $v = 246$  GeV. In the limit where  $s_l, t'_l \gg 1$ , the three light charged-lepton masses can be obtained by integrating out the heavy degrees of freedom. A straightforward calculation gives rise to an effective Yukawa matrix  $Y_\ell$  of the form

$$Y_\ell \simeq -\lambda \left[ \frac{1}{s_l - t'_l} + \frac{1}{s_l} \right]. \quad (2.9)$$

In order to assess the validity of this approximate formula, let us consider the one-generation case. Assuming  $s_l \sim t'_l$ , the determinant of  $\mathcal{M}^\ell$  is of order  $M^2 s_l v_d$ . On the other hand, the product of the singular values reads  $m_\tau M^2 s_l^2$ , where  $m_\tau$  is the tau lepton mass and the heavy partners are assumed to have a mass of order  $M s_l$ . Comparing these two expressions for  $|\text{Det } \mathcal{M}^\ell|$  provides an estimate of the magnitude of  $s_l \sim v_d/m_\tau$  which is greater than about 10 for  $\tan \beta \in [1, 15]$ . Hence,  $s_l, t'_l \gg 1$  is generally satisfied so that Eq. (2.9) provides a good approximation, even for the third generation.

The flavour structure of the charged leptons originates in the matrices  $s_l$  and  $t'_l$ . These are free parameters of the theory which, however, have to be chosen such as to yield correct charged-lepton masses. It is therefore convenient to replace  $s_l - t'_l$  in Eq. (2.7) in favour of  $Y_\ell$  using Eq. (2.9). Going to a basis in which  $Y_\ell$  is diagonal we have

$$s_l - t'_l \rightarrow - \left[ \frac{\hat{Y}_\ell}{\lambda} + s_l^{-1} \right]^{-1} = - \left[ \frac{\sqrt{2} \hat{M}^\ell}{\lambda v_d} + s_l^{-1} \right]^{-1}, \quad (2.10)$$

where hats denote diagonal  $3 \times 3$  matrices and  $\hat{M}^\ell = \text{Diag}(m_e, m_\mu, m_\tau)$  contains the measured charged-lepton masses. Having eliminated  $t'_l$  in Eq. (2.7), the charged-lepton masses are automatically correctly described, regardless of the flavour structure encoded in  $s_l$ . The latter provides the dominant source for lepton-flavour violation in our model.

---

<sup>3</sup>We use the label  $\ell$  for charged leptons while  $l$  refers to both charged and neutral leptons.

### 3 Charged-lepton flavour sector

In order to discuss the flavour phenomenology of the charged leptons, we have to express the gauge-kinetic terms in the mass basis. The procedure is analogous to the treatment of the quark sector. However there exist some simplifications due to the smallness of the tau lepton Yukawa coupling, as well as subtle differences resulting from the fact that neutrinos can be regarded as massless particles for our purposes.

#### 3.1 Diagonalising the charged-lepton mass matrix

Our starting point is the  $9 \times 9$  mass matrix of Eq. (2.7) which we rewrite using the singular value decomposition

$$s_l = V_s^\dagger \hat{s} U_s, \quad s_l - t'_l = V_t^\dagger \hat{t} U_t. \quad (3.1)$$

Here  $V_{s,t}$  and  $U_{s,t}$  are unitary matrices, while  $\hat{s}$  and  $\hat{t}$  denote the diagonalised versions of  $s_l$  and  $s_l - t'_l$ , respectively. The latter is related to the charged-lepton masses via Eq. (2.10). Hence,  $V_s$ ,  $U_s$  and  $\hat{s}$  can be regarded as free parameters, while  $V_t$ ,  $U_t$  and  $\hat{t}$  are derived from the bi-unitary diagonalisation of the right-hand side of Eq. (2.10).

In the following we briefly sketch the sequence of basis transformations which diagonalises  $\mathcal{M}^\ell$  of Eq. (2.7). More details are provided in Appendix A.1 where we follow closely the corresponding discussion in [29]. First, we absorb the  $3 \times 3$  matrices  $V_{s,t}$  and  $U_{s,t}$  into a redefinition of the fields such that the only non-diagonal blocks within  $\mathcal{M}^\ell$  are the ones proportional to  $\epsilon_d$ . As shown in Appendix A.1, the resulting matrix can be easily diagonalised in the limit of  $\epsilon_d = 0$ . Applying this basis transformations on the full mass matrix  $\mathcal{M}^\ell$  yields

$$\mathcal{M}^\ell \rightarrow \begin{pmatrix} a \epsilon_d & b \epsilon_d & 0 \\ 0 & \hat{e} & 0 \\ c \epsilon_d & d \epsilon_d & \hat{f} \end{pmatrix} M, \quad (3.2)$$

where  $a, b, c, d, \hat{e}$  and  $\hat{f}$  are  $3 \times 3$  matrices whose definition can be found in Appendix A.1. A further, more complicated transformation which block-diagonalises  $\mathcal{M}^\ell$  to second order in  $\epsilon_d$  is given explicitly in Appendix A.1. It results in the following simple form of  $\mathcal{M}^\ell$ ,

$$\mathcal{M}^\ell \rightarrow \begin{pmatrix} a \epsilon_d & 0 & 0 \\ 0 & \hat{e} + \mathcal{O}(\epsilon_d^2) & 0 \\ 0 & 0 & \hat{f} + \mathcal{O}(\epsilon_d^2) \end{pmatrix} M + \mathcal{O}(\epsilon_d^3) M. \quad (3.3)$$

The final step of the sequence of basis transformations diagonalises the upper left block  $av_d/\sqrt{2}$  of  $\mathcal{M}^\ell$ , which gives rise to the diagonal charged-lepton Yukawa coupling

$$\hat{Y}_\ell = \mathcal{V} a \mathcal{U}^\dagger. \quad (3.4)$$

The unitary  $3 \times 3$  matrices  $\mathcal{V}$  and  $\mathcal{U}$  are directly related to the parametrisation in Eq. (3.1). This becomes clear by considering the explicit form of  $a$ , which is calculated in Appendix A.1 to second order in  $\hat{s}^{-1}$  and  $\hat{t}^{-1}$ . From Eq. (A.8), together with Eq. (3.1), we get

$$a \approx -\lambda U_s (U_s^\dagger \hat{s}^{-1} V_s + U_t^\dagger \hat{t}^{-1} V_t) V_t^\dagger = -\lambda U_s \left( \frac{1}{s_l} + \frac{1}{s_l - t'_l} \right) V_t^\dagger. \quad (3.5)$$



Inserting the substitution of Eq. (2.10) shows that

$$\mathcal{V} \approx U_s^\dagger, \quad \mathcal{U} \approx V_t^\dagger. \quad (3.6)$$

These relations represent a significant simplification compared to the quark sector where  $\mathcal{V}$  and  $\mathcal{U}$  could only be determined numerically. All steps of the sequence of basis transformations are explicitly stated in Appendix A.1. They describe the change from the original flavour basis  $\Psi_{L,R}^\ell$  to the approximate mass basis  $\Psi_{L,R}'^\ell$ . Before applying these transformations to the gauge-kinetic terms, it is necessary to consider the relevant transformations in the neutral sector.

### 3.2 The neutral-lepton mass matrix

In order to study charged-lepton flavour violation, it is sufficient to treat the left-handed neutrinos in the massless limit. The advantage of this limit lies in the possibility to choose identical basis transformations for both components of the lepton doublet. However, due to the mixing with the heavy partners of the neutrinos, the massless neutral fermions do not simply correspond to  $\bar{q}_L^\nu \subset \bar{\Psi}_L^\nu$ . It is therefore necessary to scrutinise the mass matrix of the neutral fermions in more detail. In addition to the 18 neutral components of  $\bar{\Psi}_L^\nu$  and  $\Psi_R^\nu$ , the model presented in [29] introduces two further fermions  $\bar{\Theta}_L$  and  $\Theta_R$  which acquire very large Majorana masses at the flavour symmetry breaking scale  $\Lambda_\nu^{(\prime)}$ , cf. Table 1. The coupling of  $\bar{\Theta}_L$  to  $\Sigma_R$  induces a Majorana mass around the seesaw scale for the latter. Hence, integrating out  $\bar{\Theta}_L$  and  $\Theta_R$ , we obtain a bilinear mass term of the form

$$\frac{1}{2} \Psi_{\text{Maj}}^T \mathcal{M}^{\text{Maj}} \Psi_{\text{Maj}}, \quad (3.7)$$

where

$$\Psi_{\text{Maj}} = (\bar{\Psi}_L^{\nu T}, \Psi_R^\nu) = (\bar{q}_L^{\nu T}, \bar{\Sigma}_L^{\nu T}, \bar{\Xi}_L^{\nu T}, q_R^\nu, \Sigma_R^\nu, \Xi_R^\nu), \quad (3.8)$$

and

$$\mathcal{M}^{\text{Maj}} = \begin{pmatrix} 0 & 0 & 0 & 0 & 1\lambda\epsilon_u & 1 \\ 0 & 0 & 0 & 1 & s_l + t'_l & 0 \\ 0 & 0 & 0 & 1\lambda\epsilon_u & 0 & s_l \\ 0 & 1 & 1\lambda\epsilon_u & 0 & 0 & 0 \\ 1\lambda\epsilon_u & (s_l + t'_l)^T & 0 & 0 & y & 0 \\ 1 & 0 & s_l^T & 0 & 0 & 0 \end{pmatrix} M. \quad (3.9)$$

The only direct Majorana-type entry of the  $18 \times 18$  mass matrix  $\mathcal{M}^{\text{Maj}}$  is given by, cf. Appendix A.1.1 of [29],

$$y \equiv \frac{M_{\Sigma_R^\nu}}{M} = \frac{(\varphi'_\alpha \Lambda_\varphi)^2}{M \Lambda_\nu} s_\nu^{-1}. \quad (3.10)$$

In the following we intend to identify the directions of the three lightest neutral fermions. These correspond to the massless states of the limit  $\epsilon_u = 0$ . Having diagonalised the submatrix  $s_l$  of  $\mathcal{M}^{\text{Maj}}$  analogously to the charged sector by absorbing  $V_s$  and  $U_s$  into a redefinition of the fields  $q_L^\nu$  and  $\Xi_{L,R}^\nu$ , it is straightforward to rotate the  $\bar{q}_L^\nu \Xi_R^\nu$  coupling



into the  $\bar{\Xi}_L^\nu \Xi_R^\nu$  mass term. As detailed in Appendix A.2, such a basis transformation simplifies the mass matrix of Eq. (3.9), with  $\epsilon_u = 0$ , to

$$\mathcal{M}^{\text{Maj}} \Big|_{\epsilon_u=0} \rightarrow \begin{pmatrix} 0 & 0 & 0 & 0 & 0 & 0 \\ 0 & 0 & 0 & \mathbb{1} & s_l + t'_l & 0 \\ 0 & 0 & 0 & 0 & 0 & \hat{s} \\ 0 & \mathbb{1} & 0 & 0 & 0 & 0 \\ 0 & (s_l + t'_l)^T & 0 & 0 & y & 0 \\ 0 & 0 & \hat{s} & 0 & 0 & 0 \end{pmatrix} M . \quad (3.11)$$

In this basis, the first three components correspond to the massless neutrinos which decouple from the massive neutral fermions. Furthermore, we find separated Dirac pairs whose masses are given by the diagonal matrix  $\hat{s}$ ; their entries are all larger than  $M$ . The remaining degrees of freedom mix via

$$\begin{pmatrix} 0 & \mathbb{1} & s_l + t'_l \\ \mathbb{1} & 0 & 0 \\ (s_l + t'_l)^T & 0 & y \end{pmatrix} M , \quad (3.12)$$

resulting in three masses around the seesaw scale  $yM = M_{\Sigma_R^\nu}$  as well as six masses of order  $M$ . Having isolated the three massless neutrinos from the massive neutral fermions in Eq. (3.11), no further transformation which mixes light and heavy degrees of freedom must be applied on  $\Psi_{\text{Maj}}$ . The only allowed additional transformations are mixings of the three neutrinos themselves. Being massless, it is convenient to choose these identical to the corresponding unitary transformations of the charged leptons.

### 3.3 Gauge-kinetic terms

The basis transformations discussed above must now be applied to the gauge-kinetic terms. As the flavour gauge bosons are far too heavy to have an impact on experimental observables, we do not consider them in the following. On the other hand, among the PS gauge bosons, only the SM ones are relevant for low-energy phenomenology. A comprehensive discussion of the gauge-kinetic terms involving the fermionic PS multiplets can be found in [29]. In the original basis, it applies to the lepton sector without any modifications. However, the change from the flavour to the mass basis differs for quarks and leptons. We therefore have to reanalyse the flavour structure of the neutral and charged currents for leptons.

The gauge-kinetic terms involving the electroweak gauge bosons have been derived in [29]. Although we are not interested in neutral currents involving the neutrinos, we include these in the following in order to facilitate a direct comparison with the expressions

of the quark sector. In the original flavour basis, we have<sup>4</sup>

$$\begin{aligned}
\mathcal{L}_{\text{kin}} \supset & \frac{g}{c_W} \bar{\Psi}_L \left( (\tau^3 - s_W^2 Q_e) \mathbb{1} - \mathcal{K}'_L \tau^3 \right) \not{Z} \Psi_L \\
& + \frac{g}{c_W} \bar{\Psi}_R \left( -s_W^2 Q_e \mathbb{1} + \mathcal{K}_R \tau^3 \right) \not{Z} \Psi_R \\
& + \frac{g}{\sqrt{2}} \bar{\Psi}_L^\nu \mathcal{K}_L \not{W}^+ \Psi_L^\ell + \text{h.c.} \\
& + \frac{g}{\sqrt{2}} \bar{\Psi}_R^\nu \mathcal{K}_R \not{W}^+ \Psi_R^\ell + \text{h.c.} ,
\end{aligned} \tag{3.13}$$

where

$$\mathcal{K}'_L = \begin{pmatrix} 0 & 0 & 0 \\ 0 & \mathbb{1} & 0 \\ 0 & 0 & 0 \end{pmatrix} , \quad \mathcal{K}_R = \begin{pmatrix} 0 & 0 & 0 \\ 0 & 0 & 0 \\ 0 & 0 & \mathbb{1} \end{pmatrix} , \quad \mathcal{K}_L = \begin{pmatrix} \mathbb{1} & 0 & 0 \\ 0 & 0 & 0 \\ 0 & 0 & \mathbb{1} \end{pmatrix} . \tag{3.14}$$

Going to the mass basis, only the terms proportional to  $\mathcal{K}'_L$ ,  $\mathcal{K}_R$  and  $\mathcal{K}_L$  change their form. The explicit results are given in Appendix A.3. Focusing on the upper left  $3 \times 3$  blocks, we obtain

$$\begin{aligned}
\mathcal{L}_{\text{kin}} \supset & \frac{g}{c_W} \bar{\ell}_L \left( \left(-\frac{1}{2} - s_W^2 Q_e\right) \mathbb{1} + \frac{1}{2} \Delta g_{Z\bar{\ell}_L \ell_L} \right) \not{Z} \ell_L \\
& + \frac{g}{c_W} \bar{\ell}_R \left( -s_W^2 Q_e \mathbb{1} - \frac{1}{2} \Delta g_{Z\bar{\ell}_R \ell_R} \right) \not{Z} \ell_R \\
& + \frac{g}{\sqrt{2}} \bar{\nu}_L (\mathbb{1} - \Delta g_{W\bar{\nu}_L \ell_L}) \not{W}^+ \ell_L + \text{h.c.} ,
\end{aligned} \tag{3.15}$$

where the mass basis  $q_{L,R}^\ell$  and  $q_L^\nu$  has been renamed by  $\ell_{L,R}$  and  $\nu_L$ , respectively. The anomalous  $Z$  and  $W$  couplings are given as

$$\Delta g_{Z\bar{\ell}_L \ell_L} = U_t^\dagger \hat{t}^{-2} U_t \lambda^2 \epsilon_d^2 = \left[ \frac{\sqrt{2} \hat{M}^\ell}{\lambda v_d} + s_l^{-1} \right] \left[ \frac{\sqrt{2} \hat{M}^\ell}{\lambda v_d} + s_l^{-1} \right]^\dagger \lambda^2 \epsilon_d^2 , \tag{3.16}$$

$$\Delta g_{Z\bar{\ell}_R \ell_R} = V_s^\dagger \hat{s}^{-2} V_s \lambda^2 \epsilon_d^2 = [s_l^{-1}]^\dagger [s_l^{-1}] \lambda^2 \epsilon_d^2 , \tag{3.17}$$

$$\Delta g_{W\bar{\nu}_L \ell_L} = \frac{1}{2} U_t^\dagger \hat{t}^{-2} U_t \lambda^2 \epsilon_d^2 = \frac{1}{2} \left[ \frac{\sqrt{2} \hat{M}^\ell}{\lambda v_d} + s_l^{-1} \right] \left[ \frac{\sqrt{2} \hat{M}^\ell}{\lambda v_d} + s_l^{-1} \right]^\dagger \lambda^2 \epsilon_d^2 . \tag{3.18}$$

A few comments are in order. In Eq. (3.15), we have omitted the neutral currents of the neutrinos. Furthermore, we do not show the charged currents involving the right-handed neutrinos as  $q_R^\nu$  corresponds to heavy neutral fermions. Working in the limit of massless left-handed neutrinos, we do not encounter a non-trivial PMNS matrix in the corresponding charged current. Finally, note that the anomalous  $W$  coupling is related to the anomalous  $Z$  coupling by  $\Delta g_{W\bar{\nu}_L \ell_L} = \frac{1}{2} \Delta g_{Z\bar{\ell}_L \ell_L}$ .

---

<sup>4</sup>We use the standard abbreviation  $s_W = \sin \theta_W$  and  $c_W = \cos \theta_W$  for the sine and cosine of the weak mixing angle.

### 3.4 Anomalous Higgs coupling

The discussion of the anomalous coupling of the charged leptons to the Higgs proceeds analogously to the treatment of the Higgs-quark-quark coupling in Section 3.3 of [29]. It requires the basis transformation to be computed to third order in the expansion parameter  $\epsilon_d$ . Building on the results of [29], we parameterise the relevant higher-order correction by

$$\begin{aligned}\Delta g_{h\bar{\ell}\ell} &\approx -\epsilon_d^2 \left[ U_s^\dagger b \hat{e}^{-2} b^\dagger U_s \cdot \hat{Y}_\ell + \hat{Y}_\ell \cdot V_t^\dagger c^\dagger \hat{f}^{-2} c V_t \right] \\ &\approx -\lambda^2 \epsilon_d^2 \left\{ \left[ \frac{\sqrt{2}\hat{M}^\ell}{\lambda v_d} + s_l^{-1} \right] \left[ \frac{\sqrt{2}\hat{M}^\ell}{\lambda v_d} + s_l^{-1} \right]^\dagger \cdot \hat{Y}_\ell + \hat{Y}_\ell \cdot [s_l^{-1}]^\dagger [s_l^{-1}] \right\}.\end{aligned}\quad (3.19)$$

Performing the sequence of basis transformations discussed in Section 3.1, the Yukawa matrix is given by [29]

$$Y_\ell \approx \hat{Y}_\ell + \frac{1}{2} \Delta g_{h\bar{\ell}\ell}, \quad (3.20)$$

while the Higgs-lepton-lepton coupling takes the form

$$g_{h\bar{\ell}\ell} \approx \hat{Y}_\ell + \frac{3}{2} \Delta g_{h\bar{\ell}\ell}. \quad (3.21)$$

The latter is thus related to the former via

$$g_{h\bar{\ell}\ell} \approx Y_\ell + \Delta g_{h\bar{\ell}\ell}. \quad (3.22)$$

The diagonalisation of  $Y_\ell$  in Eq. (3.20) to this higher order in  $\epsilon_d$  is achieved by unitary matrices which deviate from the identity by contributions of order  $\epsilon_d^2$ . Such a basis change does not affect the second term in Eq. (3.22) at the given order. Hence, the deviation of the Higgs coupling from the diagonal charged-lepton Yukawa matrix is simply given by  $\Delta g_{h\bar{\ell}\ell}$  of Eq. (3.19).

## 4 LFV observables from effective field theory

In this section we discuss the effects of our model on the low-energy LFV observables. In particular, these are induced by flavour-changing couplings of the fermions to the SM gauge bosons ( $Z, W$ ) and Higgs particle ( $h$ ), while the couplings to the new gauge bosons ( $Z'$  etc.) are additionally suppressed due to their heavy mass, as we have already explained in [29]. Moreover, the mass scale associated with the dimension-five Weinberg operator, relevant for the neutrino masses, is much larger than the NP scale  $M$  for charged LFV in our model, and the respective heavy Majorana neutrinos decouple. The relevant operators in an effective theory at the electroweak scale can then be identified as

$$\begin{aligned}\mathcal{L}_{\text{LFV}} = & \frac{gZ^\mu}{2c_W} \left( \Delta g_{Z\bar{\ell}_L\ell_L}^{ij} (\bar{\ell}_i \gamma_\mu P_L \ell_j) - \Delta g_{Z\bar{\ell}_R\ell_R}^{ij} (\bar{\ell}_i \gamma_\mu P_R \ell_j) \right) \\ & - \frac{gW^\mu}{\sqrt{2}} \Delta g_{W\bar{\nu}_L\ell_L}^{ij} (\bar{\nu}_i \gamma_\mu P_L \ell_j) + \frac{h}{\sqrt{2}} \Delta g_{h\bar{\ell}\ell}^{ij} (\bar{\ell}_i P_R \ell_j) + \text{h.c.},\end{aligned}\quad (4.1)$$

where the  $3 \times 3$  coupling matrices  $\Delta g_{Z\bar{\ell}_L\ell_L}$ ,  $\Delta g_{Z\bar{\ell}_R\ell_R}$ ,  $\Delta g_{W\bar{\nu}_L\ell_L}$  and  $\Delta g_{h\bar{\ell}\ell}$  are given in Eqs. (3.16–3.19). The terms in Eq. (4.1) descend from the gauge-invariant dimension-six operators

$$\Phi^\dagger i \overleftrightarrow{D}^\mu \Phi (\bar{E}_i \gamma_\mu E_j), \quad \Phi^\dagger i \overleftrightarrow{D}^\mu \Phi (\bar{L}_i \gamma_\mu L_j), \quad \Phi^\dagger i \tau^A \overleftrightarrow{D}^\mu \Phi (\bar{L}_i \tau^A \gamma_\mu L_j), \quad (\Phi^\dagger \Phi) \bar{L}_i \Phi E_j,$$

appearing in the Buchmüller-Wyler Lagrangian [3,4] after electroweak symmetry breaking.

In the following, we will focus on radiative transitions of the type  $\ell_i \rightarrow \ell_f \gamma$ , tri-lepton decays  $\ell_i \rightarrow 3\ell_f$  and lepton conversion in nuclei. As the energy release of each process is typically of the order of the mass of the initial charged lepton, we consider – as usual – a low-energy effective Lagrangian where all fields with masses above the charged-lepton mass have been integrated out, notably the heavy SM gauge bosons.

## 4.1 The decay $\mu \rightarrow e \gamma$

Starting with the decay  $\mu \rightarrow e \gamma$ , we follow the conventions of [63] and consider the low-energy operators

$$\mathcal{L}_{\mu \rightarrow e \gamma} = A_R m_\mu F_{\sigma\rho} (\bar{\ell}_e \sigma^{\sigma\rho} P_R \ell_\mu) + A_L m_\mu F_{\sigma\rho} (\bar{\ell}_e \sigma^{\sigma\rho} P_L \ell_\mu) + \text{h.c.} . \quad (4.2)$$

With this definition the branching ratio of  $\mu \rightarrow e \gamma$  can be written as [63]

$$\text{Br}(\mu \rightarrow e \gamma) = \frac{m_\mu^5}{4\pi \Gamma_\mu} (|A_L|^2 + |A_R|^2) . \quad (4.3)$$

The coefficients  $A_{L/R}$  receive contributions from 1-loop diagrams involving anomalous  $Z$  and  $W$  couplings, see Fig. 1. For completeness, we have also included 2-loop diagrams of the “Barr-Zee type” [64,65] which involve the anomalous Higgs couplings as these can be dominant in some corners of parameter space. Using the results of [63], the coefficients  $A_{L/R}$  can be expressed in terms of the various anomalous couplings of Eq. (4.1), and we obtain

$$m_\mu A_R = - \frac{2Q_{\ell e}}{3(4\pi)^2 v^2} \left( s_W^2 \left[ -m_\mu \Delta g_{Z\bar{\ell}_L\ell_L}^{12} + m_e \Delta g_{Z\bar{\ell}_R\ell_R}^{12} \right] - m_\mu \Delta g_{Z\bar{\ell}_L\ell_L}^{12} - \frac{3}{2} m_e \Delta g_{Z\bar{\ell}_R\ell_R}^{12} \right. \\ \left. - \frac{5}{2} m_\mu \Delta g_{W\bar{\nu}_L\ell_L}^{12} \right) + A_{BZ} \frac{1}{\sqrt{2}} \Delta g_{h\bar{\ell}\ell}^{12} , \quad (4.4)$$

$$m_\mu A_L = - \frac{2Q_{\ell e}}{3(4\pi)^2 v^2} \left( s_W^2 \left[ -m_e \Delta g_{Z\bar{\ell}_L\ell_L}^{12} + m_\mu \Delta g_{Z\bar{\ell}_R\ell_R}^{12} \right] - m_e \Delta g_{Z\bar{\ell}_L\ell_L}^{12} - \frac{3}{2} m_\mu \Delta g_{Z\bar{\ell}_R\ell_R}^{12} \right. \\ \left. - \frac{5}{2} m_e \Delta g_{W\bar{\nu}_L\ell_L}^{12} \right) + A_{BZ} \frac{1}{\sqrt{2}} [\Delta g_{h\bar{\ell}\ell}^\dagger]^{12} , \quad (4.5)$$

where the expression for the Barr-Zee coefficient  $A_{BZ}$  can also be found in [63]. The adaptation to other transitions ( $\tau \rightarrow \mu \gamma$ ,  $\tau \rightarrow e \gamma$ ) is straightforward. Note that, in practice, all terms proportional to the electron mass  $m_e$  can be dropped in Eqs. (4.4,4.5).

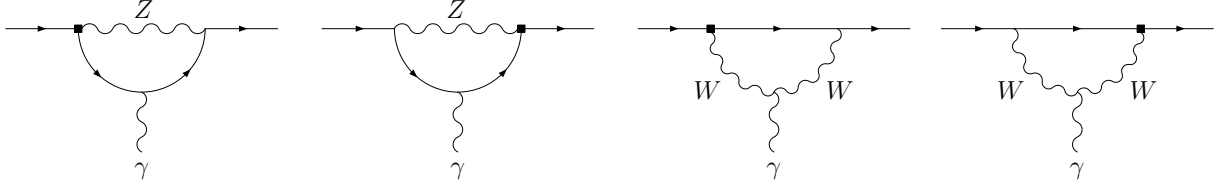


Figure 1: 1-loop topologies contributing to  $A_{L/R}$ . The black square indicates the insertion of an anomalous  $Z$  or  $W$  coupling.

## 4.2 The decay $\mu \rightarrow 3e$

Turning to the decay  $\mu \rightarrow 3e$ , we have to add to Eq. (4.2) a set of four-lepton operators (following again the notation of [63]),

$$\begin{aligned} \mathcal{L}_{\mu \rightarrow 3e} = \mathcal{L}_{\mu \rightarrow e\gamma} &+ g_1 (\bar{\ell}_e P_R \ell_\mu) (\bar{\ell}_e P_R \ell_e) + g_2 (\bar{\ell}_e P_L \ell_\mu) (\bar{\ell}_e P_L \ell_e) \\ &+ g_3 (\bar{\ell}_e \gamma^\nu P_R \ell_\mu) (\bar{\ell}_e \gamma_\nu P_R \ell_e) + g_4 (\bar{\ell}_e \gamma^\nu P_L \ell_\mu) (\bar{\ell}_e \gamma_\nu P_L \ell_e) \\ &+ g_5 (\bar{\ell}_e \gamma^\nu P_R \ell_\mu) (\bar{\ell}_e \gamma_\nu P_L \ell_e) + g_6 (\bar{\ell}_e \gamma^\nu P_L \ell_\mu) (\bar{\ell}_e \gamma_\nu P_R \ell_e) + \text{h.c.} . \end{aligned} \quad (4.6)$$

The branching ratio for  $\mu \rightarrow 3e$  can then be expressed as

$$\begin{aligned} \text{Br}(\mu \rightarrow 3e) = \frac{m_\mu^5}{1536 \pi^3 \Gamma_\mu} &\left[ \frac{|g_1|^2 + |g_2|^2}{8} + 2(|g_3|^2 + |g_4|^2) + |g_5|^2 + |g_6|^2 \right. \\ &- 8e \text{Re}[A_R(2g_4^* + g_6^*) + A_L(2g_3^* + g_5^*)] \\ &\left. + 64e^2 \left( \ln \frac{m_\mu}{m_e} - \frac{11}{8} \right) (|A_L|^2 + |A_R|^2) \right]. \end{aligned} \quad (4.7)$$

Again, the adaptation to different flavour transitions is straightforward. Notice that the coefficients  $A_{L/R}$  only arise at 1-loop level, while the couplings  $g_i$  are generated by tree-level exchange of weak gauge bosons.<sup>5</sup> However, as can be seen from Eq. (4.7),  $A_{L/R}$  come with a large pre-factor and should thus be included for completeness. Expressing the couplings  $g_i$  of the four-lepton operators in terms of the anomalous  $Z$  and  $W$  couplings to fermions of Eq. (4.1), we find

$$\begin{aligned} g_1 &\simeq g_2 \simeq 0 , \\ g_3 &= \frac{2s_W^2}{v^2} \Delta g_{Z\bar{\ell}_R \ell_R}^{12} , & g_4 &= -\frac{2s_W^2 - 1}{v^2} \Delta g_{Z\bar{\ell}_L \ell_L}^{12} , \\ g_5 &= \frac{2s_W^2 - 1}{v^2} \Delta g_{Z\bar{\ell}_R \ell_R}^{12} , & g_6 &= -\frac{2s_W^2}{v^2} \Delta g_{Z\bar{\ell}_L \ell_L}^{12} . \end{aligned} \quad (4.8)$$

<sup>5</sup>Our Pati-Salam model also generates contributions to the coefficients  $g_{1,2}$  via the anomalous Higgs coupling, which is similar to the situation in the Randall-Sundrum scenario discussed in [63]. However, as noted in [63], the associated tree-level matching diagrams are suppressed by a factor of the electron mass and can therefore be neglected.

### 4.3 Muon conversion in nuclei

Finally, the appropriate low-energy Lagrangian for muon conversion in nuclei now also contains mixed four-fermion operators with lepton and quark currents (see e.g. [66, 67]),

$$\begin{aligned}
\mathcal{L}_{\mu N \rightarrow e N} &= \mathcal{L}_{\mu \rightarrow e \gamma} \\
&+ \sum_{q=u,d,s} \frac{m_q m_\mu}{M_h^2} c_{SL}^q (\bar{\ell}_e P_R \ell_\mu) (\bar{q} q) + \sum_{q=u,d,s} \frac{m_q m_\mu}{M_h^2} c_{SR}^q (\bar{\ell}_e P_L \ell_\mu) (\bar{q} q) \\
&+ \sum_{q=u,d} c_{VL}^q (\bar{\ell}_e \gamma^\nu P_L \ell_\mu) (\bar{q} \gamma_\nu q) + \sum_{q=u,d} c_{VR}^q (\bar{\ell}_e \gamma^\nu P_R \ell_\mu) (\bar{q} \gamma_\nu q) \\
&+ \frac{\alpha_s m_\mu}{M_h^2} c_{gg}^L (\bar{\ell}_e P_R \ell_\mu) G^{A,\sigma\rho} G_{\sigma\rho}^A + \frac{\alpha_s m_\mu}{M_h^2} c_{gg}^R (\bar{\ell}_e P_L \ell_\mu) G^{A,\sigma\rho} G_{\sigma\rho}^A + \text{h.c.} \quad (4.9)
\end{aligned}$$

Here  $M_h$  denotes the SM Higgs mass. Note that in order to calculate the branching ratio for muon conversion, one also has to take into account the hadronic matrix elements of the quark and gluon operators which depend on the specific properties of the participating nucleus  $N$ . Using once again the definitions from [63], we write

$$\begin{aligned}
&\text{Br}(\mu N \rightarrow e N) \\
&= \frac{m_\mu^5}{4\Gamma_{\text{capture}}} \left| A_R \mathcal{D} + 4 \left[ \frac{m_\mu m_p}{M_h^2} \left( \tilde{C}_{SL}^p - 12\pi \tilde{C}_{L,gg}^p \right) \mathcal{S}^p + \tilde{C}_{VL}^p \mathcal{V}^p + \{p \rightarrow n\} \right] \right|^2 \\
&+ \{L \leftrightarrow R\} \quad (4.10)
\end{aligned}$$

Conventionally, the branching ratio has been normalised to the total capture rate  $\Gamma_{\text{capture}}$  of the respective nucleus  $N$ . The coefficients  $\mathcal{D}$ ,  $\mathcal{S}^{p,n}$ ,  $\mathcal{V}^{p,n}$  in Eq. (4.10) encode the properties of the target nucleus, see [68], where the superscript refers to the proton and neutron contributions, respectively. Furthermore, the coefficients  $\tilde{C}_X^p$  are given by

$$\tilde{C}_{SL}^p = \sum_{q=u,d,s} c_{SL}^q f_q^p, \quad \tilde{C}_{VL}^p = \sum_{q=u,d} c_{VL}^q f_{V_q}^p, \quad \tilde{C}_{L,gg}^p = c_{gg}^L f_Q^p, \quad (4.11)$$

and analogously for  $p \rightarrow n$  and  $L \rightarrow R$ . Here, the form factors  $f_q^{p,n}$  and  $f_{V_q}^{p,n}$  parametrise the coupling strengths of the quark scalar and vector currents of flavour  $q$  to nucleons, respectively.  $f_Q^{p,n}$  represent the scalar couplings of heavy quarks ( $c, b, t$ ). Finally, the genuine LFV effects are contained in short-distance Wilson coefficients which in the tree-level approximation read

$$c_{SL}^q = -\frac{1}{\sqrt{2}m_\mu v} \Delta g_{h\bar{\ell}\ell}^{12}, \quad c_{SR}^q = -\frac{1}{\sqrt{2}m_\mu v} [\Delta g_{h\bar{\ell}\ell}^\dagger]^{12}, \quad (4.12)$$

and

$$\begin{aligned}
c_{VL}^u &= -\frac{1}{v^2} \left[ \frac{1}{2} \Delta g_{Z\bar{\ell}_L \ell_L}^{12} \left( 1 - \frac{8}{3} s_W^2 \right) \right], \quad c_{VR}^u = \frac{1}{v^2} \left[ \frac{1}{2} \Delta g_{Z\bar{\ell}_R \ell_R}^{12} \left( 1 - \frac{8}{3} s_W^2 \right) \right], \\
c_{VL}^d &= -\frac{1}{v^2} \left[ \frac{1}{2} \Delta g_{Z\bar{\ell}_L \ell_L}^{12} \left( -1 + \frac{4}{3} s_W^2 \right) \right], \quad c_{VR}^d = \frac{1}{v^2} \left[ \frac{1}{2} \Delta g_{Z\bar{\ell}_R \ell_R}^{12} \left( -1 + \frac{4}{3} s_W^2 \right) \right], \quad (4.13)
\end{aligned}$$

as well as [69, 70]

$$c_{gg}^L = -\frac{1}{12\pi} \sum_{q=c,b,t} c_{SL}^q, \quad c_{gg}^R = -\frac{1}{12\pi} \sum_{q=c,b,t} c_{SR}^q. \quad (4.14)$$

## 5 Numerical analysis

In the previous section, we have given analytic expressions for all relevant LFV observables in terms of the anomalous coupling constants of the SM particles generated by the Pati-Salam model at low energy scales. These coupling constants depend directly on the  $3 \times 3$  flavour matrices  $s_l$  and  $t'_l$ , where the latter can be expressed in terms of  $s_l$  and the effective Yukawa matrix  $Y_\ell$  through the relation in Eq. (2.9). As such, all leptonic branching ratios discussed in Section 4 can be understood as complicated functions of the free model parameters in the matrix  $s_l$ . With hardly any restriction on the entries of this matrix, the phenomenological analysis naturally lends itself to a numerical scan over a sizeable and representative part of the parameter space. In the following, we employ two scan strategies. For the first strategy, we adopt the same ranges for the flavour-unspecific input parameters as in the analysis of quark-flavour effects performed in [29], i.e.

$$\lambda \in [1.5, 3], \quad \tan \beta \in [1, 15], \quad M \in [750, 2500] \text{ GeV}. \quad (5.1)$$

Furthermore, we choose the entries of the diagonal matrix  $\hat{s}$ , cf. Eq. (3.1), to lie within the interval  $[\frac{1}{3}, 3] \times \frac{\lambda v_d}{\sqrt{2} M \ell}$  in order to avoid too much tuning between  $t'_l$  and  $s_l$  in Eq. (2.10). The mixing angles and phases in the unitary matrices  $V_s$  and  $U_s$  in Eq. (3.1) are allowed to be arbitrarily large for this part of the numerical scan.

Our second scan strategy is based on the same ranges for  $\lambda$  and  $\tan \beta$  as in Eq. (5.1). However, the NP mass scale  $M$  is fixed at 1 TeV. Adopting the standard CKM convention to parameterise the unitary matrices  $V_s$  and  $U_s$ , we then investigate the dependence of the various LFV observables on the associated mixing angles. To this end, we generate two datasets: one dataset (blue or dark grey points) with arbitrary mixing angles, and another dataset (orange or light grey points) where the mixing angles are restricted to be small, i.e. in the range  $[0, \pi/6]$ .

In practice, we first randomly generate entries for the matrix  $s_l$ , together with the parameters  $\lambda$ ,  $\tan \beta$  and  $M$  within the above-mentioned ranges. For each set of numerical input parameters we compute the flavour matrix  $t'_l$  through Eq. (2.9) so that the measured charged-lepton masses are correctly reproduced. Each scan comprises  $10^5$  model points. For each model point, we calculate the corresponding anomalous couplings, and from these the rates for  $\mu \rightarrow e\gamma$ ,  $\mu \rightarrow 3e$ ,  $\mu \rightarrow e$  conversion as well as for the corresponding tau decays. For muon conversion, we use the same low-energy parameters as in [63]. In particular, this implies that the muon conversion is computed for a gold target nucleus. We note that the future experiment DeeMe [71] uses a silicon target, while Mu2E [72] and COMET [73] propose aluminium targets. Following the argumentation of [63], the projected upper limit for Mu2E of  $6 \times 10^{-17}$  for aluminium can be translated to a limit of about  $10^{-16}$  for gold targets.

### 5.1 Muonic decays

In order to illustrate the results of our parameter scan, we show the branching ratios of  $\mu \rightarrow e\gamma$ ,  $\mu \rightarrow 3e$  and  $\mu \rightarrow e$  conversion in form of two-dimensional scatter plots. These indicate the typical range of the branching ratios and the correlation between different observables. We stress that the point density in these scatter plots depends on the



Process	Current limit	Future limit
$\text{Br}(\mu \rightarrow e\gamma)$	$4.2 \times 10^{-13}$ [74]	$6 \times 10^{-14}$ [75]
$\text{Br}(\mu \rightarrow 3e)$	$1 \times 10^{-12}$ [76]	$1 \times 10^{-16}$ [77]
$\text{Br}^{\text{Au}}(\mu N \rightarrow eN)$	$7 \times 10^{-13}$ [78]	$1 \times 10^{-16}$ [72]

Table 2: Current and future experimental limits on the LFV branching ratios.

particular generation of random numbers, and *does not* reflect a probability distribution of the respective observable in the considered model.

Fig. 2 shows the values of the branching ratios for  $\mu \rightarrow e\gamma$ ,  $\mu \rightarrow 3e$  and muon conversion as a function of the NP scale  $M$ . Each plot contains the current and future experimental upper limits, see Table 2, visualised by solid and dashed lines, respectively. All three plots show the expected scaling of the branching fractions with the small parameter  $\epsilon_d^4 \propto 1/M^4$ . We observe that the resulting branching ratios for the decay  $\mu \rightarrow e\gamma$  are largely compatible with the experimental upper bound, even after taking into account the proposed future upgrade of the MEG experiment [75]. The small values for the  $\mu \rightarrow e\gamma$  branching ratio can be explained by the one-loop suppression of the effective Wilson coefficients relevant to this decay in our model. In contrast, the  $\mu \rightarrow 3e$  decay and  $\mu \rightarrow e$  conversion are induced by tree-level processes which lead to larger effects, and thus the present and future experimental bounds cut stronger into the NP parameter space. Especially in the case of muon conversion, with the anticipated future sensitivity, our model could lead to clear LFV signals.

To investigate the specific role of the mixing angles in the matrices  $U_s$  and  $V_s$  and the correlations between the different LFV branching ratios, we display in Fig. 3 the correlations between  $\mu \rightarrow e\gamma$  and  $\mu \rightarrow 3e$ ,  $\mu \rightarrow e\gamma$  and  $\mu N \rightarrow eN$ , as well as  $\mu \rightarrow 3e$  and  $\mu N \rightarrow eN$  for a fixed NP scale,  $M = 1$  TeV. Orange (light grey) points mark models where the mixing angles in Eq. (3.1) are restricted to values smaller than  $\pi/6$ , while blue (dark grey) points indicate the scenario with arbitrary mixing angles. A common feature of all three plots is that the restriction to small mixing angles also leads to smaller branching ratios.<sup>6</sup> This is easily explained by the general increase of the anomalous coupling constants with larger mixing angles. As both  $\mu \rightarrow 3e$  and  $\mu N \rightarrow eN$  are generated by tree-level contributions to the same kind of Wilson coefficients, both processes are strongly correlated, a feature also known from other LFV models where the dipole operators are suppressed compared to the 4-fermion operators (see for instance the Randall-Sundrum scenario with the Higgs field localised on the UV-brane as discussed in [63, 79]). On the other hand, the loop-induced decay  $\mu \rightarrow e\gamma$  shows only weak correlations with both  $\mu \rightarrow 3e$  and  $\mu N \rightarrow eN$ . These generic features of the LFV phenomenology distinguish our model from other extensions of the SM such as Little Higgs models (see e.g. [80–83]), supersymmetric scenarios (see e.g. [84–91]), left-right symmetric models (see e.g. [92]) or models with a fourth fermion generation (see e.g. [93]).

---

<sup>6</sup>Note that the points with small mixing angles conceal most of the model points with arbitrary mixing angles in the correlation plots.

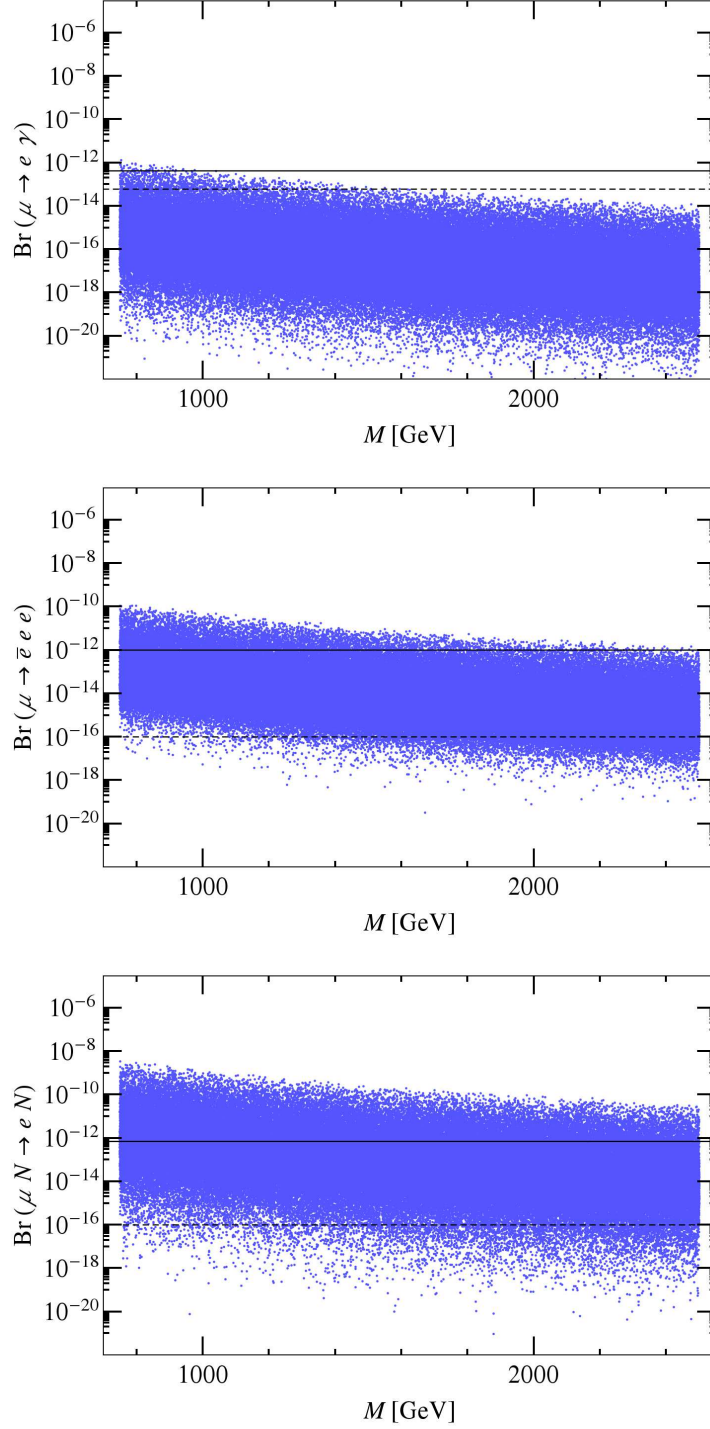


Figure 2: Scatter plots of the branching ratios for  $\mu \rightarrow e \gamma$  (top),  $\mu \rightarrow 3e$  (centre) and  $\mu \rightarrow e$  conversion (bottom) as a function of the NP scale  $M$ . The solid (dashed) lines indicate the current (future) experimental limits.

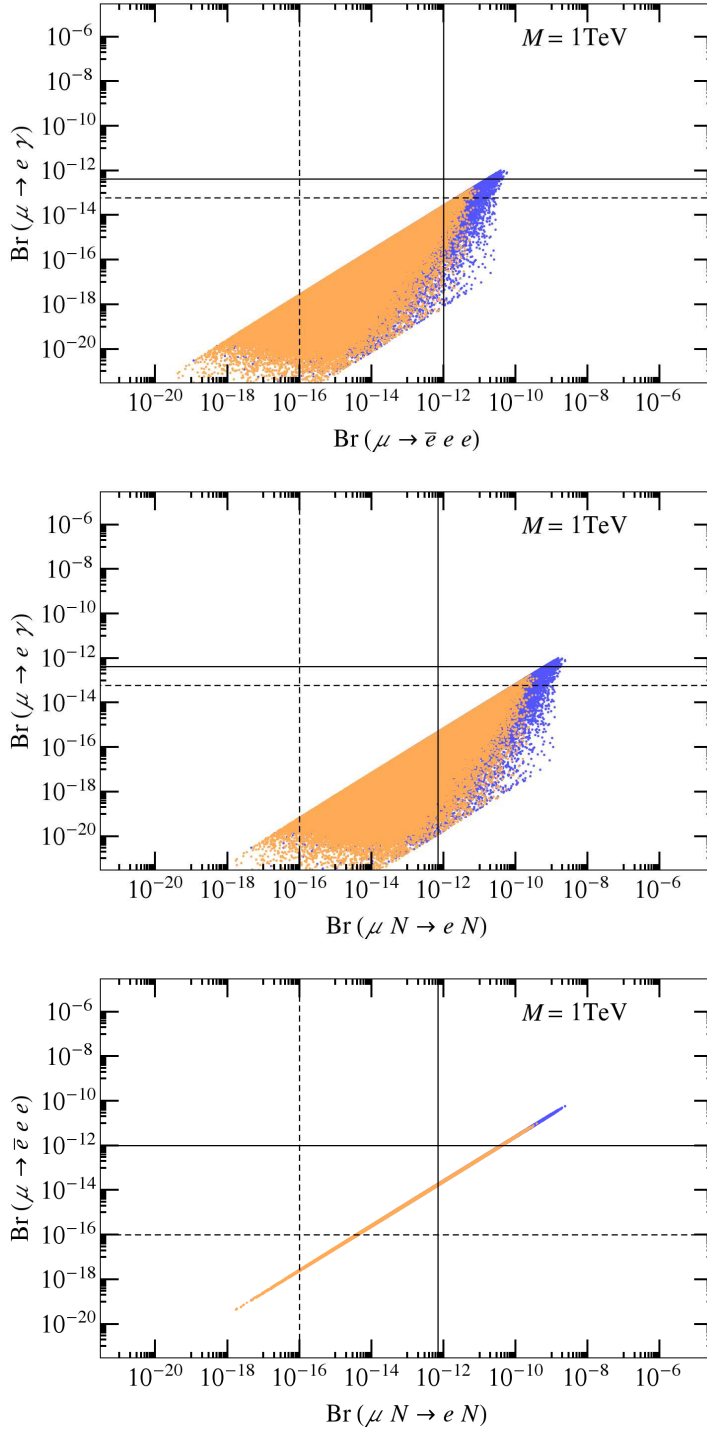


Figure 3: Correlation between the branching ratios for  $\mu \rightarrow e \gamma$  vs.  $\mu \rightarrow 3e$  (top),  $\mu \rightarrow e \gamma$  vs.  $\mu N \rightarrow e N$  (centre) as well as  $\mu \rightarrow 3e$  vs.  $\mu N \rightarrow e N$  (bottom). Each plot shows the results for a fixed NP scale,  $M = 1$  TeV. The scenario with arbitrary mixing angles is displayed with blue (dark grey) points, while the scenario with mixing angles smaller than  $\pi/6$  is shown with orange (light grey) points. (Orange points are plotted on top of blue points.)

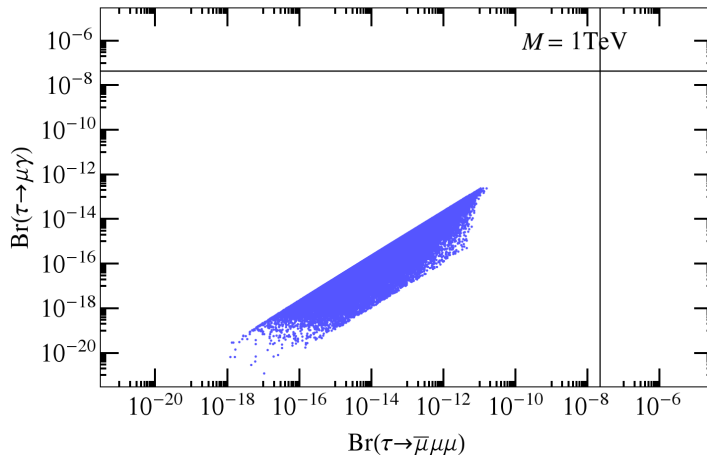


Figure 4: Correlation between the branching ratios of  $\tau \rightarrow \mu\gamma$  and  $\tau \rightarrow 3\mu$  for a fixed NP scale,  $M=1$  TeV.

## 5.2 LFV tau decays and the electron EDM

In addition to the muon sector, the decays of the tau lepton offer another opportunity to observe LFV. However the  $\tau$  is not suitable for low-energy experiments due to its high mass and short lifetime. The best bounds on processes like  $\tau \rightarrow \mu\gamma$  have been obtained at the BaBar [94], Belle [95] and LHCb [96] experiments. The solid lines in Fig. 4 show the current experimental limits,

$$\text{Br}(\tau \rightarrow \mu\gamma) < 4.4 \times 10^{-8} \quad [94] , \quad (5.2)$$

$$\text{Br}(\tau \rightarrow 3\mu) < 2.1 \times 10^{-8} \quad [95] , \quad (5.3)$$

which can be compared to the predictions of our model for the corresponding branching ratios with  $M = 1$  TeV, displayed by the blue points (again referring to the scenario with arbitrary mixing angles for  $V_s$  and  $U_s$  in Eq. (3.1)). Compared to the corresponding muonic case, the plot in Fig. 4 shows a similar correlation. However, the predicted values for the branching ratios are at least three magnitudes smaller than the best upper limits and will not be accessible in the near future.

We conclude the discussion of the lepton-flavour phenomenology in our model by considering the strong experimental constraints on the electron electric dipole moment (EDM). Using the above low-energy Lagrangian, the electron EDM can be directly calculated via (see e.g. [63])

$$d_e = m_e i (A_R - A_L). \quad (5.4)$$

However, up to terms proportional to  $\mathcal{O}(\epsilon_d^2)$ , the anomalous coupling matrices, generated by the Pati-Salam model at low energies, are hermitian. Thus, the diagonal elements are real, and our setup does not generate any contributions to the EDM at one-loop level, as long as we restrict ourselves to the insertion of only one anomalous coupling, i.e. the effect of dimension-six operators. This raises the question whether dimension-eight terms

could provide significant contributions to the electron EDM. To estimate the effects of such dimension-eight operators, we have calculated diagrams of the type shown in Fig. 1 with two anomalous gauge boson couplings instead of one. Formally, such diagrams correspond to dimension-eight contributions where the imaginary part does not vanish for two external electron states with, for instance, a  $Z$  boson exchanged inside the loop. We find that such a diagram contributes to the electron EDM only by a numerically negligible amount which, for all points of our dataset, is at least two orders of magnitude smaller than the measured upper limit [97]

$$|d_e| < 8.7 \cdot 10^{-29} e \text{ cm} . \quad (5.5)$$

Assuming normal power counting, we thus conjecture that the contributions of other dimension-eight operators to the electron EDM will be parametrically suppressed in a similar manner.

## 6 Conclusions

We have shown how the Pati-Salam model with gauged  $SU(3)_I \times SU(3)_{II}$  flavour symmetry constructed in [29] can be extended to yield a realistic description of the charged-lepton flavour sector. It requires a non-trivial extension of the flavour symmetry breaking scalar sector, involving VEVs of flavon fields which transform non-trivially with respect to the Pati-Salam symmetry group. The model features two heavy fermionic partners for each SM fermion, whose mixing with the charged leptons gives rise to anomalous couplings with the SM gauge bosons as well as the Higgs boson. Expressing the low-energy effective Lagrangian in terms of these anomalous couplings, we have determined the branching ratios for  $\mu \rightarrow e\gamma$ ,  $\mu \rightarrow 3e$ ,  $\mu \rightarrow e$  conversion as well as for the corresponding tau decays both analytically and numerically.

Our phenomenological analysis shows that, for the bulk of parameter space of the model, we do not expect to see any experimental evidence for the decay  $\mu \rightarrow e\gamma$  in the near future. This is similar to other LFV models in which the decay is only induced at the one-loop level. On the other hand,  $\mu \rightarrow 3e$  decays and  $\mu \rightarrow e$  conversion in nuclei are induced by tree-level processes in our setup. This entails branching ratios which are accessible with future experimental sensitivity, provided the new-physics scale associated to the heavy fermions in our model is of the order of a few TeV. Moreover, for the parameter range assumed in our scans, we found that both branching ratios are highly correlated.

In the case of lepton-flavour violating  $\tau$  decays, we found that the branching ratios predicted within our model turn out to be orders of magnitude smaller than the corresponding current experimental limits. Similarly, contributions to the electron EDM are parametrically suppressed and safely below the present experimental bound.

In conclusion, our particular model setup, which combines the idea of grand unification in the gauge sector and flavour symmetry breaking transferred by new heavy vector-like fermions, leads to small flavour-violating effects in the charged-lepton sector, without imposing the concept of minimal flavour violation in the technical sense (as defined in [11],

see also the critical discussion in [98]). In particular, the neutrino sector with the phenomenology of the PMNS matrix is completely decoupled from LFV in the charged-lepton sector.

## Acknowledgements

This work is supported by the Deutsche Forschungsgemeinschaft (DFG) within the Research Unit FOR 1873 (“Quark Flavour Physics and Effective Field Theories”).

## Appendix

### A Details of required basis transformations

#### A.1 Diagonalising the charged-lepton mass matrix

In Section 3.1, we have only sketched the diagonalisation of the  $9 \times 9$  mass matrix of the charged leptons as defined in Eq. (2.7). Here, we fill in the gaps by explicitly defining the individual steps [labelled by a subscript ( $i$ )] of the sequence of basis transformations. We follow closely the discussion in Appendix C of [29].

1. Basis with diagonal  $Y_\ell = \hat{Y}_\ell$ :

We begin with  $\mathcal{M}^\ell$  of Eq. (2.7) in a basis where  $Y_\ell$ , as defined in Eq. (2.9), is diagonal. Generally, neither  $s_l$  nor  $s_l - t'_l$  will be diagonal in that basis. We therefore rewrite these two matrices using the singular value decomposition of Eq. (3.1).

2. Diagonalising  $s_l$  and  $s_l - t'_l$ :

Next, we apply the basis transformation

$$\bar{\Psi}_{L(2)}^\ell = \bar{\Psi}_{L(1)}^\ell \text{diag}(U_s^\dagger, V_t^\dagger, V_s^\dagger), \quad \Psi_{R(2)}^\ell = \text{diag}(V_t, U_t, U_s) \Psi_{R(1)}^\ell, \quad (\text{A.1})$$

so that

$$\mathcal{M}_{(2)}^\ell = \begin{pmatrix} 0 & U^\dagger \lambda \epsilon_d & \mathbf{1} \\ \mathbf{1} & \hat{t} & 0 \\ V^\dagger \lambda \epsilon_d & 0 & \hat{s} \end{pmatrix} M, \quad (\text{A.2})$$

with

$$U^\dagger = U_s U_t^\dagger, \quad V^\dagger = V_s V_t^\dagger. \quad (\text{A.3})$$

The matrices  $\hat{s}$  and  $\hat{t}$  are the diagonal versions of  $s_l$  and  $s_l - t'_l$ , see Eq. (3.1). The structure of Eq. (A.2) is identical to the one of Eq. (C.2) in [29]. Therefore, we can simply follow the sequence of basis transformations described in Appendix C of [29].

3. Diagonalising  $\mathcal{M}_{(2)}^\ell$  for  $\epsilon_d = 0$ :

With vanishing  $\epsilon_d$ , the three generations do not mix with each other. It is therefore straightforward to diagonalise  $\mathcal{M}_{(2)}^\ell$  in this limit by introducing the following matrices of cosines and sines

$$\hat{c}_x = \text{diag}(c_x^1, c_x^2, c_x^3), \quad \hat{s}_x = \text{diag}(s_x^1, s_x^2, s_x^3), \quad (\text{A.4})$$

where

$$c_x^i = \frac{\hat{x}_i}{\sqrt{1 + \hat{x}_i^2}}, \quad s_x^i = \frac{1}{\sqrt{1 + \hat{x}_i^2}}, \quad (\text{A.5})$$

and  $x = s, t$ . Defining the basis transformation

$$\overline{\Psi}_{L(3)}^\ell \approx \overline{\Psi}_{L(2)}^\ell \begin{pmatrix} \hat{c}_s & 0 & \hat{s}_s \\ 0 & \mathbb{1} & 0 \\ -\hat{s}_s & 0 & \hat{c}_s \end{pmatrix}, \quad \Psi_{R(3)}^\ell \approx \begin{pmatrix} \hat{c}_t & -\hat{s}_t & 0 \\ \hat{s}_t & \hat{c}_t & 0 \\ 0 & 0 & \mathbb{1} \end{pmatrix} \Psi_{R(2)}^\ell, \quad (\text{A.6})$$

diagonalises  $\mathcal{M}_{(2)}^\ell$  in the limit where  $\epsilon_d = 0$ . Reinstating non-vanishing  $\epsilon_d$  yields the mass matrix  $\mathcal{M}_{(3)}^\ell$  which is of the form as given in Eq. (3.2). The exact form of the  $3 \times 3$  submatrices  $a, b, c, d, \hat{e}$  and  $\hat{f}$  was derived in [29]. In this work, we can simplify these expressions thanks to the small Yukawa coupling of the tau lepton, and hence  $\hat{x}_i \gg 1$ . Expanding to second order in  $\hat{x}_i^{-1}$  we have

$$\hat{c}_x \approx \mathbb{1} - \frac{1}{2}\hat{x}^{-2}, \quad \hat{s}_x \approx \hat{x}^{-1}, \quad (\text{A.7})$$

and with it

$$a \approx -(\hat{s}^{-1}V^\dagger + U^\dagger\hat{t}^{-1})\lambda, \quad (\text{A.8})$$

$$b \approx (U^\dagger - \hat{s}^{-1}V^\dagger\hat{t}^{-1} - \frac{1}{2}\hat{s}^{-2}U^\dagger - \frac{1}{2}U^\dagger\hat{t}^{-2})\lambda, \quad (\text{A.9})$$

$$c \approx (V^\dagger - \hat{s}^{-1}U^\dagger\hat{t}^{-1} - \frac{1}{2}\hat{s}^{-2}V^\dagger - \frac{1}{2}V^\dagger\hat{t}^{-2})\lambda, \quad (\text{A.10})$$

$$d \approx (V^\dagger\hat{t}^{-1} + \hat{s}^{-1}U^\dagger)\lambda, \quad (\text{A.11})$$

$$\hat{e} \approx \hat{t}, \quad (\text{A.12})$$

$$\hat{f} \approx \hat{s}. \quad (\text{A.13})$$

#### 4. Block-diagonalising $\mathcal{M}_{(3)}^\ell$ up to order $\epsilon_d^2$ :

The matrix in Eq. (3.2) can be block-diagonalised (to second order in  $\epsilon_d$ ) by

$$\overline{\Psi}_{L(4)}^\ell \equiv \overline{\Psi}_{L(3)}^\ell [\mathcal{R}_{12}(\xi_{12}^\ell)]^\dagger [\mathcal{R}_{23}(\xi_{23}^\ell)]^\dagger [\mathcal{R}_{13}(\xi_{13}^\ell)]^\dagger, \quad (\text{A.14})$$

$$\Psi_{R(4)}^\ell \equiv [\mathcal{R}_{12}(\xi_{12}^\ell)] [\mathcal{R}_{23}(\xi_{23}^\ell)] [\mathcal{R}_{13}(\xi_{13}^\ell)] \Psi_{R(3)}^\ell. \quad (\text{A.15})$$

Here  $\mathcal{R}_{\alpha\beta}(\xi)$  denotes a “rotation in the  $\alpha$ - $\beta$  plane”, expanded to second order in  $\xi$ . For example,

$$\mathcal{R}_{12}(\xi) = \begin{pmatrix} \mathbb{1} - \frac{1}{2}\xi\xi^\dagger & -\xi & 0 \\ \xi^\dagger & \mathbb{1} - \frac{1}{2}\xi^\dagger\xi & 0 \\ 0 & 0 & \mathbb{1} \end{pmatrix}, \quad (\text{A.16})$$



while the other two rotations are identical up to obvious permutations of rows and columns. In terms of the parameters of Eq. (3.2), the  $3 \times 3$  matrices  $\xi$  and  $\zeta$  have already been derived in [29],

$$\xi_{12}^\ell = b\hat{e}^{-1}\epsilon_d, \quad [\xi_{23}^\ell]_{ij} = \frac{-\hat{e}_i d_{ij}^\dagger}{\hat{e}_i^2 - \hat{f}_j^2} \epsilon_d, \quad \xi_{13}^\ell = ac^\dagger \hat{f}^{-2} \epsilon_d^2, \quad (\text{A.17})$$

$$\zeta_{12}^\ell = a^\dagger b \hat{e}^{-2} \epsilon_d^2, \quad [\zeta_{23}^\ell]_{ij} = \frac{-d_{ij}^\dagger \hat{f}_j}{\hat{e}_i^2 - \hat{f}_j^2} \epsilon_d, \quad \zeta_{13}^\ell = c^\dagger \hat{f}^{-1} \epsilon_d. \quad (\text{A.18})$$

Inserting the expressions of Eqs. (A.8–A.13) and keeping only terms up to second order in  $\hat{s}^{-1}$  and  $\hat{t}^{-1}$ , we find for the charged leptons

$$\xi_{12}^\ell \approx U^\dagger \hat{t}^{-1} \lambda \epsilon_d, \quad [\xi_{23}^\ell]_{ij} \approx \frac{-V_{ij} - \hat{t}_i U_{ij} \hat{s}_j^{-1}}{\hat{t}_i^2 - \hat{s}_j^2} \lambda \epsilon_d, \quad \xi_{13}^\ell \approx 0, \quad (\text{A.19})$$

$$\zeta_{12}^\ell \approx 0, \quad [\zeta_{23}^\ell]_{ij} \approx \frac{-\hat{t}_i^{-1} V_{ij} \hat{s}_j - U_{ij}}{\hat{t}_i^2 - \hat{s}_j^2} \lambda \epsilon_d, \quad \zeta_{13}^\ell \approx V \hat{s}^{-1} \lambda \epsilon_d. \quad (\text{A.20})$$

With this result, the basis change in Eqs. (A.14,A.15) simplifies to

$$\begin{aligned} [\mathcal{R}_{12}(\xi_{12}^\ell)]^\dagger [\mathcal{R}_{23}(\xi_{23}^\ell)]^\dagger &\approx \begin{pmatrix} \mathbb{1} - \frac{1}{2} \xi_{12}^\ell \xi_{12}^{\ell\dagger} & \xi_{12}^\ell & 0 \\ -\xi_{12}^{\ell\dagger} & \mathbb{1} - \frac{1}{2} \xi_{12}^{\ell\dagger} \xi_{12}^\ell & 0 \\ 0 & 0 & \mathbb{1} \end{pmatrix} \begin{pmatrix} \mathbb{1} & 0 & 0 \\ 0 & \mathbb{1} & \xi_{23}^\ell \\ 0 & -\xi_{23}^{\ell\dagger} & \mathbb{1} \end{pmatrix} \\ &\approx \begin{pmatrix} \mathbb{1} - \frac{1}{2} \xi_{12}^\ell \xi_{12}^{\ell\dagger} & \xi_{12}^\ell & 0 \\ -\xi_{12}^{\ell\dagger} & \mathbb{1} - \frac{1}{2} \xi_{12}^{\ell\dagger} \xi_{12}^\ell & \xi_{23}^\ell \\ 0 & -\xi_{23}^{\ell\dagger} & \mathbb{1} \end{pmatrix}, \end{aligned} \quad (\text{A.21})$$

$$\begin{aligned} [\mathcal{R}_{23}(\zeta_{23}^\ell)] [\mathcal{R}_{13}(\zeta_{13}^\ell)] &\approx \begin{pmatrix} \mathbb{1} & 0 & 0 \\ 0 & \mathbb{1} & -\zeta_{23}^\ell \\ 0 & \zeta_{23}^{\ell\dagger} & \mathbb{1} \end{pmatrix} \begin{pmatrix} \mathbb{1} - \frac{1}{2} \zeta_{13}^\ell \zeta_{13}^{\ell\dagger} & 0 & -\zeta_{13}^\ell \\ 0 & \mathbb{1} & 0 \\ \zeta_{13}^{\ell\dagger} & 0 & \mathbb{1} - \frac{1}{2} \zeta_{13}^{\ell\dagger} \zeta_{13}^\ell \end{pmatrix} \\ &\approx \begin{pmatrix} \mathbb{1} - \frac{1}{2} \zeta_{13}^\ell \zeta_{13}^{\ell\dagger} & 0 & -\zeta_{13}^\ell \\ 0 & \mathbb{1} & -\zeta_{23}^\ell \\ \zeta_{13}^{\ell\dagger} & \zeta_{23}^{\ell\dagger} & \mathbb{1} - \frac{1}{2} \zeta_{13}^{\ell\dagger} \zeta_{13}^\ell \end{pmatrix}. \end{aligned} \quad (\text{A.22})$$

The resulting mass matrix  $\mathcal{M}_{(4)}^\ell$  is given explicitly in Eq. (3.3).

##### 5. The approximate mass basis:

The final step in our sequence of basis transformations diagonalises the upper left block  $av_d/\sqrt{2}$  of  $\mathcal{M}_{(4)}^\ell$ . As discussed in Section 3.1, this requires

$$\overline{\Psi}_{L(5)}^\ell = \overline{\Psi}_{L(4)}^\ell \text{diag}(U_s, \mathbb{1}, \mathbb{1}), \quad \Psi_{R(5)}^\ell = \text{diag}(V_t^\dagger, \mathbb{1}, \mathbb{1}) \Psi_{R(4)}^\ell. \quad (\text{A.23})$$

## A.2 The neutral-lepton mass matrix

Considering the neutral fermions of the Pati-Salam model, we do not aim at a full diagonalisation of the  $18 \times 18$  Majorana mass matrix of Eq. (3.9). Yet, we must identify the correct light neutrino mass eigenstates which become massless in the limit of  $\epsilon_u = 0$ . Working in this limit, we apply a basis transformations on  $\Psi_{\text{Maj}}$  of Eq. (3.8) such that

$$\overline{\Psi}_{L(3)}^{\nu T} = \begin{pmatrix} \hat{c}_s & 0 & -\hat{s}_s \\ 0 & \mathbb{1} & 0 \\ \hat{s}_s & 0 & \hat{c}_s \end{pmatrix} \begin{pmatrix} U_s^* & 0 & 0 \\ 0 & \mathbb{1} & 0 \\ 0 & 0 & V_s^* \end{pmatrix} \overline{\Psi}_{L(1)}^{\nu T}, \quad (\text{A.24})$$

$$\Psi_{R(3)}^{\nu} = \begin{pmatrix} \mathbb{1} & 0 & 0 \\ 0 & \mathbb{1} & 0 \\ 0 & 0 & U_s \end{pmatrix} \Psi_{R(1)}^{\nu}. \quad (\text{A.25})$$

Adopting the expansion of Eq. (A.7), the mass matrix  $\mathcal{M}_{(3)}^{\text{Maj}}|_{\epsilon_u=0}$  takes the form of Eq. (3.11), in which the three massless left-handed neutrinos have already been isolated. The fourth step in the sequence of basis transformations must not be applied to the neutral sector as it would add a component of the heavy fermions to the massless particles; hence,  $\xi_{ij}^{\nu} = 0$ . Finally, the fifth step only mixes the massless neutral fermions and can be chosen identical to the corresponding unitary matrix of the charged leptons. We therefore define

$$\overline{\Psi}_{L(5)}^{\nu T} = \text{diag}(U_s^T, \mathbb{1}, \mathbb{1}) \overline{\Psi}_{L(3)}^{\nu T}. \quad (\text{A.26})$$

We do not specify the transformations of the heavy neutral fermions as they are practically irrelevant for charged-lepton flavour violating observables involving only the electron, the muon and the tau lepton.

## A.3 Non-standard gauge-kinetic couplings

In the neutral currents of the charged leptons, deviations from the Standard Model originate from the terms of Eq. (3.13) which are proportional to  $\mathcal{K}'_L$  and  $\mathcal{K}_R$ . Applying the sequence of basis transformations defined in Appendix A.1 yields

$$\mathcal{K}'_{L(5)}{}^0 = \begin{pmatrix} U_s^\dagger \xi_{12}^\ell \xi_{12}^{\ell \dagger} U_s & -U_s^\dagger \xi_{12}^\ell & 0 \\ -\xi_{12}^{\ell \dagger} U_s & 1 - \xi_{12}^{\ell \dagger} \xi_{12}^\ell & \xi_{23}^\ell \\ 0 & \xi_{23}^{\ell \dagger} & 0 \end{pmatrix}, \quad (\text{A.27})$$

$$\mathcal{K}_{R(5)}^0 = \begin{pmatrix} V_t^\dagger \zeta_{13}^\ell \zeta_{13}^{\ell \dagger} V_t & 0 & -V_t^\dagger \zeta_{13}^\ell \\ 0 & 0 & -\zeta_{23}^\ell \\ -\zeta_{13}^{\ell \dagger} V_t & -\zeta_{23}^{\ell \dagger} & 1 - \zeta_{13}^{\ell \dagger} \zeta_{13}^\ell \end{pmatrix}, \quad (\text{A.28})$$

with  $\xi_{ij}^\ell$  and  $\zeta_{ij}^\ell$  given in Eqs. (A.19,A.20).

Turning to the charged current involving the left-handed neutrino, we have not fully specified the transformation which diagonalises the mass matrix of all neutral fermions. In particular, we have skipped the diagonalisation of the Majorana mass matrix of Eq. (3.12). Therefore, we will only determine the upper left  $3 \times 3$  block of  $\mathcal{K}_{L(5)}^+$  which describes the

anomalous coupling of the  $W$  to the light SM leptons. It is easy to see that a change from the original basis of the charged and neutral leptons to the corresponding third basis, as defined in Eqs. (A.1,A.6,A.24), does not modify the matrix  $\mathcal{K}_L$  at all. Performing the transformations of Eqs. (A.21,A.23,A.26) to the final mass basis, one can derive the following form for the upper left  $3 \times 3$  block of  $\mathcal{K}_{L(5)}^+$ ,

$$U_s^\dagger \left( \mathbf{1} - \frac{1}{2} \xi_{12}^\ell \xi_{12}^{\ell \dagger} \right) U_s, \quad (\text{A.29})$$

where  $\xi_{12}^\ell$  is given in Eq. (A.19).

## References

- [1] G. Aad *et al.* [ATLAS Collaboration], Phys. Lett. B **716** (2012) 1 [arXiv:1207.7214].
- [2] S. Chatrchyan *et al.* [CMS Collaboration], Phys. Lett. B **716** (2012) 30 [arXiv:1207.7235].
- [3] W. Buchmüller and D. Wyler, Nucl. Phys. B **268** (1986) 621.
- [4] B. Grzadkowski, M. Iskrzynski, M. Misiak and J. Rosiek, JHEP **1010** (2010) 085 [arXiv:1008.4884].
- [5] R. Alonso, E. E. Jenkins, A. V. Manohar and M. Trott, JHEP **1404** (2014) 159 [arXiv:1312.2014].
- [6] W. Altmannshofer, PoS FPCP **2015** (2015) 001.
- [7] R. S. Chivukula and H. Georgi, Phys. Lett. B **188** (1987) 99.
- [8] L. J. Hall and L. Randall, Phys. Rev. Lett. **65** (1990) 2939.
- [9] A. J. Buras, P. Gambino, M. Gorbahn, S. Jäger and L. Silvestrini, Phys. Lett. B **500** (2001) 161 [hep-ph/0007085].
- [10] G. D’Ambrosio, G. F. Giudice, G. Isidori and A. Strumia, Nucl. Phys. B **645** (2002) 155 [hep-ph/0207036].
- [11] V. Cirigliano, B. Grinstein, G. Isidori and M. B. Wise, Nucl. Phys. B **728** (2005) 121 [hep-ph/0507001].
- [12] T. Feldmann, M. Jung and T. Mannel, Phys. Rev. D **80** (2009) 033003 [arXiv:0906.1523].
- [13] R. Alonso, M. B. Gavela, L. Merlo and S. Rigolin, JHEP **1107** (2011) 012 [arXiv:1103.2915].
- [14] E. Nardi, Phys. Rev. D **84** (2011) 036008 [arXiv:1105.1770].

- [15] R. Alonso, M. B. Gavela, D. Hernandez and L. Merlo, Phys. Lett. B **715** (2012) 194 [arXiv:1206.3167].
- [16] J. R. Espinosa, C. S. Fong and E. Nardi, JHEP **1302** (2013) 137 [arXiv:1211.6428].
- [17] R. Alonso, M. B. Gavela, D. Hernandez, L. Merlo and S. Rigolin, JHEP **1308** (2013) 069 [arXiv:1306.5922].
- [18] R. Alonso, M. B. Gavela, G. Isidori and L. Maiani, JHEP **1311** (2013) 187 [arXiv:1306.5927].
- [19] R. Alonso de Pablo, arXiv:1307.1904.
- [20] C. S. Fong and E. Nardi, Phys. Rev. D **89** (2014) 036008 [arXiv:1307.4412].
- [21] L. Merlo, arXiv:1503.03282.
- [22] B. Grinstein, M. Redi and G. Villadoro, JHEP **1011** (2010) 067 [arXiv:1009.2049].
- [23] M. E. Albrecht, T. Feldmann and T. Mannel, JHEP **1010** (2010) 089 [arXiv:1002.4798].
- [24] R. T. D'Agnolo and D. M. Straub, JHEP **1205** (2012) 034 [arXiv:1202.4759].
- [25] F. Bishara, A. Greljo, J. F. Kamenik, E. Stamou and J. Zupan, JHEP **1512** (2015) 130 [arXiv:1505.03862].
- [26] T. Feldmann, JHEP **1104** (2011) 043 [arXiv:1010.2116].
- [27] D. Guadagnoli, R. N. Mohapatra and I. Sung, JHEP **1104** (2011) 093 [arXiv:1103.4170].
- [28] R. N. Mohapatra, AIP Conf. Proc. **1467** (2012) 7 [arXiv:1205.6190].
- [29] T. Feldmann, F. Hartmann, W. Kilian and C. Luhn, JHEP **1510** (2015) 160 [arXiv:1506.00782].
- [30] G. Krnjaic and D. Stolarski, JHEP **1304** (2013) 064 [arXiv:1212.4860].
- [31] R. Franceschini and R. N. Mohapatra, JHEP **1304** (2013) 098 [arXiv:1301.3637].
- [32] M. C. Chen and K. T. Mahanthappa, Int. J. Mod. Phys. A **18** (2003) 5819 [hep-ph/0305088].
- [33] S. F. King, Rept. Prog. Phys. **67** (2004) 107 [hep-ph/0310204].
- [34] R. N. Mohapatra and A. Y. Smirnov, Ann. Rev. Nucl. Part. Sci. **56** (2006) 569 [hep-ph/0603118].
- [35] K. S. Babu, arXiv:0910.2948.
- [36] G. Altarelli and F. Feruglio, Rev. Mod. Phys. **82** (2010) 2701 [arXiv:1002.0211].

- [37] S. F. King and C. Luhn, Rept. Prog. Phys. **76** (2013) 056201 [arXiv:1301.1340].
- [38] S. F. King, A. Merle, S. Morisi, Y. Shimizu and M. Tanimoto, New J. Phys. **16** (2014) 045018 [arXiv:1402.4271].
- [39] S. F. King, J. Phys. G **42** (2015) 123001 [arXiv:1510.02091].
- [40] J. C. Pati and A. Salam, Phys. Rev. D **8** (1973) 1240.
- [41] J. C. Pati and A. Salam, Phys. Rev. D **10** (1974) 275 [Phys. Rev. D **11** (1975) 703].
- [42] W. Kilian and J. Reuter, Phys. Lett. B **642** (2006) 81 [hep-ph/0606277].
- [43] R. Howl and S. F. King, Phys. Lett. B **652** (2007) 331 [arXiv:0705.0301].
- [44] L. Calibbi, L. Ferretti, A. Romanino and R. Ziegler, Phys. Lett. B **672** (2009) 152 [arXiv:0812.0342].
- [45] F. Braam, J. Reuter and D. Wiesler, AIP Conf. Proc. **1200** (2010) 458 [arXiv:0909.3081].
- [46] V. De Romeri, M. Hirsch and M. Malinsky, Phys. Rev. D **84** (2011) 053012 [arXiv:1107.3412].
- [47] C. Arbelaez, R. M. Fonseca, M. Hirsch and J. C. Romão, Phys. Rev. D **87** (2013) 075010 [arXiv:1301.6085].
- [48] C. Arbelaez, M. Hirsch, M. Malinsky and J. C. Romão, Phys. Rev. D **89** (2014) 035002 [arXiv:1311.3228].
- [49] F. Hartmann, W. Kilian and K. Schnitter, JHEP **1405** (2014) 064 [arXiv:1401.7891].
- [50] S. F. King and G. G. Ross, Phys. Lett. B **574** (2003) 239 [hep-ph/0307190].
- [51] S. F. King and M. Malinsky, JHEP **0611** (2006) 071 [hep-ph/0608021].
- [52] S. F. King and M. Malinsky, Phys. Lett. B **645** (2007) 351 [hep-ph/0610250].
- [53] S. F. King and C. Luhn, Nucl. Phys. B **820** (2009) 269 [arXiv:0905.1686].
- [54] B. Dutta, Y. Mimura and R. N. Mohapatra, JHEP **1005** (2010) 034 [arXiv:0911.2242].
- [55] S. F. King and C. Luhn, Nucl. Phys. B **832** (2010) 414 [arXiv:0912.1344].
- [56] R. de Adelhart Toorop, F. Bazzocchi and L. Merlo, JHEP **1008** (2010) 001 [arXiv:1003.4502].
- [57] P. S. Bhupal Dev, R. N. Mohapatra and M. Severson, Phys. Rev. D **84** (2011) 053005 [arXiv:1107.2378].
- [58] I. de Medeiros Varzielas, JHEP **1201** (2012) 097 [arXiv:1111.3952].

- [59] P. S. Bhupal Dev, B. Dutta, R. N. Mohapatra and M. Severson, Phys. Rev. D **86** (2012) 035002 [arXiv:1202.4012].
- [60] F. Hartmann and W. Kilian, Eur. Phys. J. C **74** (2014) 3055 [arXiv:1405.1901].
- [61] S. F. King, JHEP **1408** (2014) 130 [arXiv:1406.7005].
- [62] H. Georgi and C. Jarlskog, Phys. Lett. B **86** (1979) 297.
- [63] M. Beneke, P. Moch and J. Rohrwild, Nucl. Phys. B **906** (2016) 561 [arXiv:1508.01705].
- [64] S. M. Barr and A. Zee, Phys. Rev. Lett. **65** (1990) 21 [Phys. Rev. Lett. **65** (1990) 2920].
- [65] D. Chang, W. S. Hou and W. Y. Keung, Phys. Rev. D **48** (1993) 217 [hep-ph/9302267].
- [66] Y. Kuno and Y. Okada, Rev. Mod. Phys. **73** (2001) 151 [hep-ph/9909265].
- [67] A. Crivellin, M. Hoferichter and M. Procura, Phys. Rev. D **89** (2014) 054021 [arXiv:1312.4951].
- [68] R. Kitano, M. Koike and Y. Okada, Phys. Rev. D **66** (2002) 096002 [Phys. Rev. D **76** (2007) 059902] [hep-ph/0203110].
- [69] M. A. Shifman, A. I. Vainshtein and V. I. Zakharov, Phys. Lett. B **78** (1978) 443.
- [70] A. Crivellin, M. Hoferichter and M. Procura, Phys. Rev. D **89** (2014) 093024 [arXiv:1404.7134].
- [71] M. Aoki [DeeMe Collaboration], AIP Conf. Proc. **1441** (2012) 599.
- [72] R. M. Carey *et al.* [Mu2e Collaboration], FERMILAB-PROPOSAL-0973.
- [73] Y. G. Cui *et al.* [COMET Collaboration], KEK-2009-10.
- [74] A. M. Baldini *et al.* [MEG Collaboration], arXiv:1605.05081.
- [75] A. M. Baldini *et al.*, arXiv:1301.7225.
- [76] U. Bellgardt *et al.* [SINDRUM Collaboration], Nucl. Phys. B **299** (1988) 1.
- [77] N. Berger [Mu3e Collaboration], Nucl. Phys. Proc. Suppl. **248-250** (2014) 35.
- [78] W. H. Bertl *et al.* [SINDRUM II Collaboration], Eur. Phys. J. C **47** (2006) 337.
- [79] K. Agashe, A. E. Blechman and F. Petriello, Phys. Rev. D **74** (2006) 053011 [hep-ph/0606021].
- [80] M. Blanke, A. J. Buras, B. Duling, A. Poschenrieder and C. Tarantino, JHEP **0705** (2007) 013 [hep-ph/0702136].

- [81] F. del Aguila, J. I. Illana, M. D. Jenkins, JHEP **0901** (2009) 080 [arXiv:0811.2891].
- [82] M. Blanke, A. J. Buras, B. Duling, S. Recksiegel, C. Tarantino, Acta Phys. Polon. **B41** (2010) 657 [arXiv:0906.5454].
- [83] T. Goto, Y. Okada, Y. Yamamoto, Phys. Rev. **D83** (2011) 053011 [arXiv:1012.4385].
- [84] J. R. Ellis, J. Hisano, M. Raidal and Y. Shimizu, Phys. Rev. **D66** (2002) 115013 [hep-ph/0206110].
- [85] A. Brignole, A. Rossi, Nucl. Phys. **B701** (2004) 3 [hep-ph/0404211].
- [86] P. Paradisi, JHEP **0602** (2006) 050 [hep-ph/0508054].
- [87] P. Paradisi, JHEP **0608** (2006) 047 [hep-ph/0601100].
- [88] L. Calibbi, M. Frigerio, S. Lavignac and A. Romanino, JHEP **0912** (2009) 057 [arXiv:0910.0377].
- [89] F. Feruglio, C. Hagedorn, Y. Lin and L. Merlo, Nucl. Phys. **B832** (2010) 251 [arXiv:0911.3874].
- [90] M. Dimou, S. F. King and C. Luhn, JHEP **1602** (2016) 118 [arXiv:1511.07886].
- [91] M. Dimou, S. F. King and C. Luhn, Phys. Rev. D **93** (2016) 075026 [arXiv:1512.09063].
- [92] C. H. Lee, P. S. Bhupal Dev and R. N. Mohapatra, Phys. Rev. D **88** (2013) 093010 [arXiv:1309.0774].
- [93] A. J. Buras, B. Duling, T. Feldmann, T. Heidsieck and C. Promberger, JHEP **1009** (2010) 104 [arXiv:1006.5356].
- [94] B. Aubert *et al.* [BaBar Collaboration], Phys. Rev. Lett. **104** (2010) 021802 [arXiv:0908.2381].
- [95] K. Hayasaka *et al.*, Phys. Lett. B **687** (2010) 139 [arXiv:1001.3221].
- [96] R. Aaij *et al.* [LHCb Collaboration], Phys. Lett. B **724** (2013) 36 [arXiv:1304.4518].
- [97] J. Baron *et al.* [ACME Collaboration], Science **343** (2014) 269 [arXiv:1310.7534].
- [98] S. Davidson and F. Palorini, Phys. Lett. B **642** (2006) 72 [hep-ph/0607329].